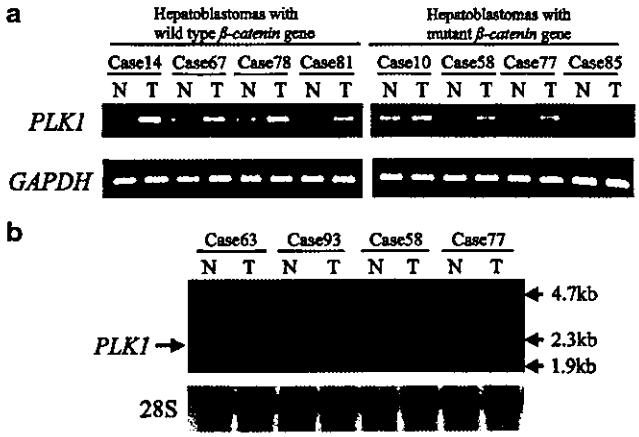

Figure 2 Increased expression of *PLK1* in HBLs. (a) Semiquantitative RT–PCR of *PLK1* gene in eight HBL cases. Preferential expression of the *PLK1* was seen in all sample pairs with and without *β-catenin* mutation. (b) Northern blot analysis of *PLK1* in primary HBLs, The 28S ribosomal band is shown as a control of each RNA amount .

nuclear protein gene *RAN*, *PLK1* onocgene, and two cholesterol metabolism-associated protein genes, *low-density lipoprotein (LDL) receptor 1* and *Niemann-Pick disease type C1 (NPC1)*. The RAN protein is involved in the control of nucleo-cytoplasmic traffic of many nuclear proteins through formation of the transport nuclear pore complex (Ribbeck *et al.*, 1998). Nagata *et al.* (2003) also reported that *RAN* is upregulated in HBLs by oligonucleotide DNA array experiment. The LDL receptor 1 binds LDL, a major plasma cholesterol-carrying lipoprotein, and plays an important role in cholesterol homeostasis (Sudhof *et al.*, 1987; Goldstein and Brown, 1990; Hamanaka *et al.*, 1992). *NPC1* is a causal gene of Niemann–Pick type C disease which is an autosomal recessive lipid storage disorder that affects the viscera and central nervous system (Brady *et al.*, 1989). It encodes a protein with sequence similarity to the morphogen receptor 'patched', and to the cholesterol-sensing regions of 3-hydroxy-3-methylglutaryl coenzyme A (HMG-CoA) reductase (Loftus *et al.*, 1997) and is involved in the intracellular trafficking of cholesterol. Concerning the differentially expressed genes which contained unknown sequences, those cDNA sequences have been submitted to the public database (Genbank/DDBJ Accession numbers: AB07 3346-AB073347, AB073382-AB073387, AB073599-AB0 73614, and AB075869-AB075881). Interestingly, only one known gene, *lymphocyte alpha-kinase (LAK)*, showed distinct expression pattern between HBLs with mutant *β-catenin* and those with wild type *β-catenin* (Figure 1a).

We next examined expression pattern of the novel genes in human multiple tissues by semi-quantitative RT–PCR and found that at least five genes were specifically expressed in the liver (a part of the data is shown in Figure 1b). Since the oncogene *PLK1* (*polo-like kinase-1*) was expressed in HBLs at significantly high levels as compared with the corresponding normal livers, we further examined the role of its expression in HBL.

PLK1 oncogene is overexpressed in HBLs

Recent studies have demonstrated that the preferential expression of *PLK1* mRNA is associated with some cancers including non-small-cell lung cancer (Wolf *et al.*, 1997), squamous cell carcinoma of the head and neck (Knecht *et al.*, 1999), and esophageal carcinoma (Tokumitsu *et al.*, 1999). However, the role of *PLK1* in HBL has never been reported. As indicated by semi-quantitative RT–PCR described above, we found that *PLK1* mRNA expression in HBLs is higher than in normal livers (Figure 2a). Northern blot analysis also confirmed its higher expression in HBLs (Figure 2b). We also performed Southern blot analysis by using the genomic DNAs obtained from primary HBLs and human placenta as a control, and probed with the *PLK1*-specific DNA fragment. However, we failed to find any clue of rearrangements or amplification of the *PLK1* gene locus (data not shown).

To examine the clinical significance of the expression level of *PLK1*, we performed quantitative real-time RT–PCR analysis using 74 primary hepatoblastomas and 29 corresponding normal liver samples (Figure 3a). The average arbitrary values of *PLK1* expression in HBLs and normal livers were 28.9 ± 6.7 and 4.1 ± 0.76, respectively (mean $\pm$ s.e.m., $P < 0.01$). The average values in alive and dead cases were 21.7 ± 5.2 ($n = 61$) and 62.4 ± 28.2 ($n = 13$), respectively ($p = 0.021$). When we compared the expression levels of *PLK1* between 24-paired HBLs and their corresponding normal livers, the former in HBL samples was significantly higher in comparison with the latter ($P < 0.01$) (Figure 3b). We also examined the relationship between the expression levels of *PLK1* and clinicopathological data of HBLs. Statistically significant correlation was observed only between histology and *PLK1* expression ($p = 0.041$). The expression level of *PLK1* in the tumors with poorly differentiated histology was higher than those with the well-differentiated one. The other clinicopathological factors such as age, clinical stage, and *β-catenin* mutation did not show a statistical significance with *PLK1* expression.

To further examine whether the *PLK1* expression was associated with the outcome of the patients with HBL, we performed a Kaplan–Meier analysis (Figure 4). The distinction between high and low levels of *PLK1* expression was based on the median value (low, *PLK1* < 13 d.u.; high, *PLK1* $\geq$ 13 d.u.). Since the overall survivals of 15 out of 74 cases were unknown, 59 cases were applied to the analysis. The 5-year survival rates of the groups with high and low *PLK1* expression were 55.9 and 87.0%, respectively ($P = 0.042$). The univariate analysis showed that both *PLK1* expression ($P = 0.015$) and histology ($P = 0.025$) have a significant prognostic importance (Table 4). The multivariate analysis demonstrated that *PLK1* expression was significantly related to survival, after controlling *β-catenin* mutation, age, stage,

Table 3 The known genes differentially expressed between hepatoblastomas and normal livers

	Gene symbol	*Acc. no*	*Gene name*
Protein synthesis, metabolism, transport			
T>N	RAN	NM_006325	GTP-binding nuclear protein RAN
N>T	LBP	AF105067	Lipopolysaccharide-binding protein
N>T	TDO2	BC005355	Tryptophan 2,3-dioxygenase
N>T	CRP	X56692	C-reactive protein
N>T	GC	NM_000583	Group-specific component
N>T	HP	K01763	Haptoglobin
N>T	HPX	NM_000613	Hemopexin
N>T	SQSTM1	NM_003900	Sequestosome 1
N>T	PHDGH	AF171237	A2-53-73 3-phosphoglycerate dehydrogenase
N>T	PPP1R3C	XM_005398	Protein phosphatase 1, regulatory (inhibitor) subunit 3C
N>T	ITIH4	D38595	Inter-alpha-trypsin inhibitor family heavy chain-related protein
N>T	G1P2	M13755	Interferon-induced 17-kDa/15-kDa protein
Cytokine, growth factor, hormones			
N>T	HABP2	D49742	Hyaluronan binding protein 2
N>T	IGFBP3	NM_000598	Insulin-like growth factor binding protein 3
N>T	GOT1	AF052153	Glutamic-oxaloacetic transaminase 1
Cell signaling			
N>T	CSNK2B	M30448	Casein kinase II, beta polypeptide
N>T	TPD52	NM_005079	Tumor protein D52
cell cycle			
T>N	PLK1	X73458	PLK1
Cell structure, adhesion			
N>T	LRG	AF403428	Leucine-rich alpha-2-glycoprotein
N>T	PGRP-L	AF384856	Peptidoglycan recognition protein L precursor
N>T	CLDN4	NM_001305	Claudin4
N>T	VTN	NM_000638	Vitronection
Organism defense			
N>T	RODH-4	NM_003708	Retinol dehydrogenase 4
N>T	MASP1	AF284421	Mannan-binding lectin serine protease 1
N>T	C4BPA	M31452	Complement component 4 binding protein, alpha
Glycometabolism			
N>T	ADH1B	AF153821	Alcohol dehydrogenase 1B, beta polypeptide
N>T	ALDOB	M15657	Aldolase B
Lipid metabolism			
T>N	NPC1	NM_000271	Niemann–Pick disease, type C1
T>N	OLR1	NM_002543	Oxidized low density lipoprotein (lectin-like) receptor 1
N>T	DGAT2	AF384161	Diacylglycerol acyltransferase
N>T	SCP2	NM_002979	Sterol carrier protein 2
N>T	APOA5	AF202890	Apolipoprotein A-V
N>T	AADAC	L32179	Arylacetamide deacetylase
N>T	SAA4	M81349	Amyloid A protein
Transcription			
N>T	BZW1	NM_014670	Basic leucine zipper and W2 domains 1
N>T	CREB-H	NM_032607	CREB/ATF family transcription factor
RNA biogenesis, metabolism			
N>T	HNRPDL	AB017018	Heterogeneous nuclear ribonucleoprotein D-like
Homeostasis, heat shock protein, metabolic enzymes			
N>T	UGT1A	AF297093	UGT1 gene locus
N>T	ALPL	X14174	Liver-type alkaline phosphatase
N>T	SLC10A1	L21893	Solute carrier family 10
N>T	CES1	AF177775	Carboxylestelase
N>T	AKR1D1	Z28339	Aldo-keto reductase family 1, member D1
N>T	AKR1C2	U05598	Aldo-keto reductase family 1, member C2
N>T	CP	D45045	Ceruloplasmin
Others			
N>T	DGCR6L	NM_033257	DiGeorge syndrome critical region gene 6 like
N>T	A1BG	AF414429	Alpha-1-B glycoprotein

T>N: highly expressed in the tumors as compared to normal livers. N>T: highly expressed in normal livers as compared to the tumors

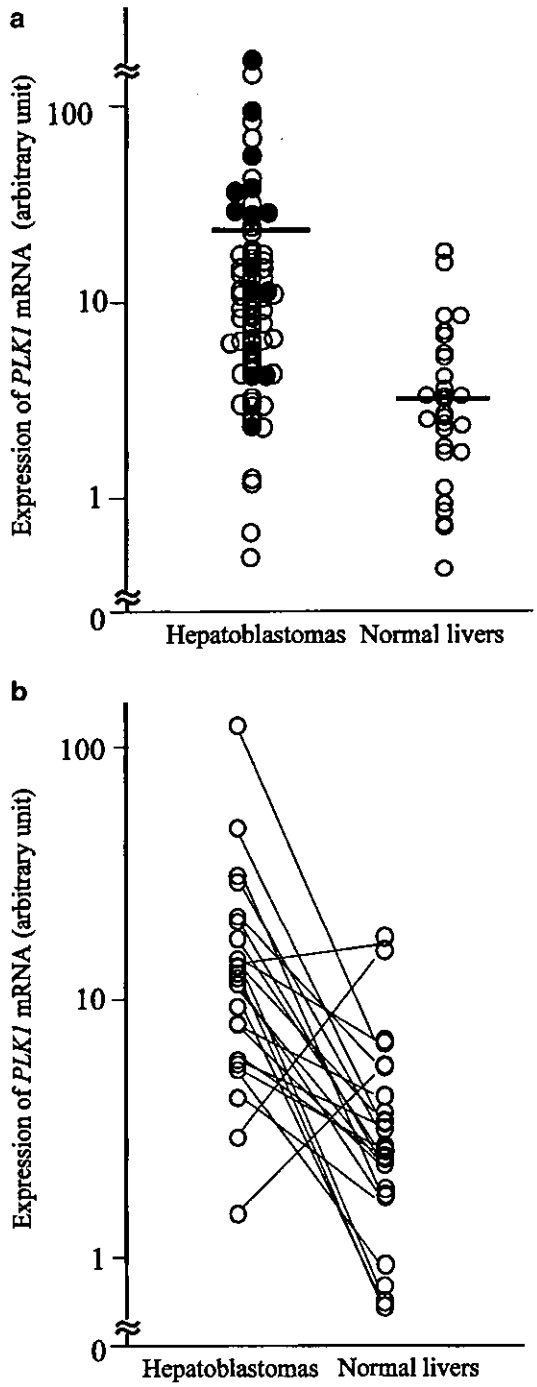

Figure 3 mRNA expression of *PLK1* in HBLs and the corresponding normal livers measured by quantitative real-time RT-PCR. (**a**) The levels of *PLK1* mRNA expression in HBLs and normal livers. The expression levels of *PLK1* were determined by quantitative real-time RT–PCR analysis using 74 HBL tissues and 29 normal livers (see Materials and methods). The *PLK1* expression values were normalized by *GAPDH*. Open and closed circles represent alive and dead, respectively. Since the values of the *PLK1* expression were skewed, a log transformation was used for the expression values. The bars show mean values. (**b**) Correlation of *PLK1* expression between HBL and its corresponding normal liver in 24 paired samples

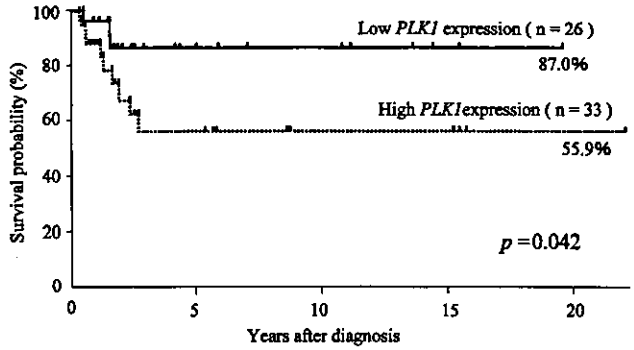

Figure 4 Kaplan–Meier survival curves ($n = 59$) in relation to the expression levels of *PLK1* (median cutoff). The arbitrary median cutoff value was set as 13. The patients with high expression of *PLK1* represented significantly poor prognosis than those with its low expression

Table 4 Univariate Cox regression analysis using *PLK1*(log) and dichotomous factors of *β-catenin* mutation, age, stage, and histology ($n = 59$)

Factor	n	P-*value*	*HR (95% CI)*
PLK1(log)	59	0.015	1.62 (1.10, 2.40)
β-catenin (mutant vs wild type)	58	0.27	1.85 (0.62, .5.56)
Age (>1 vs ≤1 year)	55	0.76	1.22 (0.33, 4.52)
Stage (3, 4 vs 1, 2)	56	0.083	3.81 (0.84, 17.2)
Histology (poorly vs well)	53	0.025	4.48 (1.21, 16.6)

All variables with two categories, except *PLK1*(log); HR = hazard ratio shows the relative of death of first category relative to second; CI = confidence interval

or histology, but marginally related to survival after controlling both histology and stage (Table 5).

Discussion

HBL is one of the embryonal tumors in close relation to the normal as well as abnormal tissue development. To understand the molecular basis of the genesis of HBL, here we randomly cloned a large number of genes expressed in HBLs with or without AFP production and in a non-tumorous infant's liver. Extensive screening for the differentially expressed genes between the tumors and their corresponding normal livers has successfully identified at least 86 genes including 40 with unknown function, which may potentially contribute to develop new therapeutic strategies against HBLs with poor prognosis.

HBL cDNA libraries

We have identified the genes with unknown function in approximately 8% of the total 10431 clones obtained from our oligo-capping cDNA libraries. The comparison of the frequently appeared genes in each libraries shows that expression profile is relatively similar between AFP-positive HBL and the normal part of the infant's liver, whereas it is very different between AFP-positive and AFP-negative tumors, in which many genes

Table 5 Multivariable Cox regression analysis using *PLK1*(log) and dichotomous factors of *β-catenin* mutation, age, stage, and histology ($n = 50$)

Variable	P-*value*	*Variable*	P-*value*	*Variable*	P-*value*
PLK1(log)	0.009	*β-catenin* (mutant vs. wild type)	0.51		
PLK1(log)	0.005	Age (>1 vs ≤1 year)	0.92		
PLK1(log)	0.019	Stage (3, 4 vs 1, 2)	0.46		
PLK1(log)	0.027	Histology (poorly vs well)	0.12		
PLK1(log)	0.052	Histology (poorly vs well)	0.12	Stage (3, 4 vs 1, 2)	0.47

All variables with two categories, except *PLK1*(log)

are downregulated (Table 2). In the library of the latter tumor, *vimentin*, *RNA-binding motif protein*, *Wnt inhibitory factor-1*, *dickkopf*, and *RAP1B* are frequently appeared, whereas they are hardly appeared in the other libraries. Wissmann *et al.* (2003) have recently reported that *WIF1* is downregulated in various cancers (prostate cancer, breast cancer, non-small-cell lung cancer, and bladder cancer), and suggested that loss of WIF1 expression may be an early event in tumorigenesis in those tissues. It is notable that, in contrast to AFP-positive HBLs, the patient's outcome of the tumor with negative AFP is very poor, though the incidence of the latter tumor is low (von Schweinitz *et al.*, 1995). This suggests that AFP-positive and AFP-negative HBLs have a different genetic as well as biological background. In addition, recent reports have demonstrated that frequent mutation of the *β-catenin* gene and nuclear accumulation of its protein product are one of the main causes of the tumorigenesis of HBL. The *APC* and *Axin* genes are also mutated in some HBLs (Oda *et al.*, 1996; Miao *et al.*, 2003; Thomas *et al.*, 2003), indicating that Wnt signaling pathway plays an important role in causing the tumors, most of which are AFP-positive. Therefore, the poor-prognostic HBL without producing AFP might be caused by the particular mechanism additional to or other than the abnormality of Wnt signaling pathway. Although the appearance frequency of the genes in each library does not always reflect the actual expression levels of each gene, it may at least in part show the differences among the tumor subsets with different genetic abnormalities. As our libraries contain many genes involved in liver development, normal liver functions, and carcinogenesis, they must be useful for making a liver-proper cDNA microarray to analyse expression profiles of HBL, viral infection-induced hepatitis, liver cirrhosis, and HCC.

Differentially expressed genes between HBLs and the corresponding normal livers

cDNA microarray, which is often applied to a comprehensive gene expression analysis, is able to detect many genes that are differentially expressed between tumors and normal tissues (Okabe *et al.*, 2001; Nagata *et al.*, 2003). However, it is expensive and needs further confirmation of the selected genes by a semi-quantitative RT–PCR or a real-time RT–PCR method. Therefore, using semi-quantitative RT–PCR and the specific primers of 1188 cDNAs, we have identified 86 genes differentially expressed between HBLs and their corresponding normal livers. Surprisingly, 75 out of 86 genes are preferentially expressed in the latter tissues, and only 11 including *RAN*, *PLK1*, *NPC1*, and *OLR1* known genes are expressed at high levels in HBLs. One of the reasons of this result may be that many gene products, which are necessary for full function in the matured liver metabolism, are dispensable for the malignant growth of the tumor except for the very limited genes. The results of some differentially expressed genes are consistent with those in the previous reports. von Horn *et al.* (2001) have shown that the mRNA levels of *insulin-like growth factor-binding proteins* including *IGFBP-3* are decreased in HBLs than in normal livers. Kinoshita and Miyata (2002) have also reported that *aldolase B* mRNA is downregulated in over 50% of 20 HCCs examined. They proposed that the measurement of aldolase activity in serum is useful to determine the number of collapsed hepatic cells in cirrhosis. Recently, evidences suggest that not only mutant β-catenin but also wild-type β-catenin localize in the cellular nuclei of HBL as well as some other cancers (Rimm *et al.*, 1999; Takayasu *et al.*, 2001). The increased expression of the *Ran* gene in HBLs might be correlated with the shuttling of β-catenin and/or other related proteins between cytoplasm and nucleus in the tumor cells.

Owing to constitutive activation of Wnt signaling in most of the HBLs, the 86 genes differentially expressed between the tumor and its corresponding normal liver were expected to contain downstream target genes of Wnt signaling pathway that might regulate early stage of the hepatic development. In this study, however, only the *lymphocyte alpha-kinase* (*LAK*) gene was found to be differentially expressed at high levels in HBLs with wild-type *β-catenin* and at low levels in those with *β-catenin* mutation. LAK is a new class of protein kinases with a novel catalytic domain, but its precise function is currently unknown (Ryazanov *et al.*, 1999). Thus, our result may suggest that the target genes of the Wnt signaling pathway are commonly affected in HBLs, regardless of the presence or absence of *β-catenin* mutation.

PLK1 as a prognostic indicator of HBL

PLK1 (*polo-like kinase 1*), the human counterpart of *polo* in *Drosophila melanogaster* and of *CDC5* in *Saccharomyces cerevisiae*, encodes a serine/threonine kinase with polo-box domains (Clay *et al.*, 1993). PLK1 is crucial for various events of mitotic progression including centrosome maturation (Lane and Nigg,

1996), spindle function (Glover *et al.*, 1996), activation of cyclin B/Cdc2 (Qian *et al.*, 1998; Toyoshima-Morimoto *et al.*, 2001), and regulation of anaphase-promoting complex (Kotani *et al.*, 1998; Nigg, 1998). Elevated expression of *PLK1* is also found in different types of adult cancers including non-small-cell lung cancer, head and neck tumors, esophageal carcinomas, melanomas, and colorectal cancers (Wolf *et al.*, 1997; Knecht *et al.*, 1999; Tokumitsu *et al.*, 1999; Dietzmann *et al.*, 2001; Takai *et al.*, 2001), implying its critical role in tumorigenesis. In the present study, we have found that *PLK1* is upregulated in primary HBLs, and that its mRNA expression levels are significantly correlated with poor outcome of the patients. Multivariate Cox regression analysis indicated that *PLK1* expression could be an independent prognostic factor from *β-catenin* mutation, age, stage, or histology. However, clinical stage did not show a significant correlation with *PLK1* expression, though it is one of the critical prognostic markers. One of the possible reasons may be that the 59 tumors we used for statistical analysis include two unusual patients, one had stage 4 tumor with good prognosis and another case had stage 1 tumor with poor prognosis. These might have reduced the significance of the tumor stage in patients' survival in our sample set.

It is notable that, among the 1188 genes we have screened for differential expression, *PLK1* is the only one known oncogene overexpressed in the HBL tissues. Smith *et al.* (1997) have reported that constitutive expression of *PLK1* in NIH3T3 cells causes oncogenic focus formation and forms tumors in nude mice. Furthermore, Liu and Erikson (2003) have recently shown that the application of small interfering RNA which specifically depletes *PLK1* expression in cancer cells inhibits cell proliferation, arrests cell cycle, and induces apoptosis. Thus, PLK1 may play a crucial role in causing HBL and other cancers. It may be interesting to examine whether *PLK1* is a target of β-catenin transported from the cytosol into the nucleus. The disruption of PLK1 function could be a future therapeutic tool for the aggressive type of hepatoblastomas.

In conclusion, our HBL cDNA project has provided a large number of genes related to liver development, metabolism, and carcinogenesis. We are currently applying these genes to the cDNA microarray system. Our cDNA resource should be an important tool to understand the molecular mechanism of the genesis of HBL as well as to develop new diagnostic and therapeutic strategies against the aggressive tumors in the future.

Materials and methods

Clinical materials

Tumor tissues and their corresponding normal liver tissues were frozen at the time of surgery and stored at −80°C until use. All specimens were provided from the Tissue Bank of the Japanese Study Group for Pediatric Liver Tumor (JPLT) (Uotani *et al.*, 1998). A total of 74 HBL samples (seven were classified as being stage 1, 17 as stage 2, 26 as stage 3, 15 as stage 4, and nine were unknown stages) were used in this study. The tumors were staged according to the Japanese histopathological classification of HBL (Hata, 1990). From 1991 to 1999, HBLs had been treated by combination chemotherapy using cisplatin and THP-adriamycin according to the JPLT-1 protocol (Sasaki *et al.*, 2002). After 2000, a more intensive chemotherapeutic regimen, ITEC (ifosfamide, THP-adriamycin, etoposide, and carboplatin), has been utilized for tumors that prove resistant to the combination chemotherapy in the JPLT-2 study. Among the 74 tumor samples we examined, 36 and 35 tumor tissues were obtained prior to and after chemotherapy, respectively, and the remaining three were unknown. In the same sample set, 59 tumors were accompanied by outcome information and used for making survival curves, among which 31 and 28 tissues were obtained prior to and after chemotherapy, respectively. Tumor histology was also classified according to Hata (1990). 'Poor histology' indicates 'poorly differentiated (embryonal type)', and 'well histology' indicates 'well-differentiated (fetal type)'. The informed consents were obtained in each institution or hospital. High molecular weight DNA and total RNA of these samples were prepared as described previously (Ichimiya *et al.*, 1999).

Construction of oligo-capping cDNA libraries

Four oligo-capping cDNA libraries, two (HMFT, HYST) derived from HBLs with secretion of AFP, one (HKMT) from HBL without AFP secretion, and one (HMFN) from the corresponding normal liver, were constructed according to the method previously described (Suzuki *et al.*, 1997). These were approved by the institutional review board. The oligo-capping method enables full-length cDNA cloning with high efficiency. The 12 000 cDNA clones in total were randomly picked up and single-run sequencing was performed. Nucleotide sequence of both ends for each cDNA clone was homology-searched against the public nucleotide database using the BLAST program at the National Center for Biotechnology Information (NCBI) (Genbank release 122, January 2001).

Differential screening of the genes by semi-quantitative RT–PCR

The eight samples were selected as PCR templates to screen for the differentially expressed genes. Cases 58 and 81 were defined as stage 2 HBL, cases 10, 67, 78, and 85 were in stage 3, case 14 was in stage 4. Among those eight tumors, four (cases 14, 67, 78, and 81) had the mutant *β-catenin*, and the others (cases 10, 58, 77, and 85) not. Mutation analysis for *β-catenin* was performed as described previously (Takayasu *et al.*, 2001). The differential expression of the genes between the HBL and normal livers was confirmed at least twice using semi-quantitative RT–PCR. The individual gene-specific PCR primer sequences were determined by using Primer3 program (provided at Washington University). For cDNA templates, 5 μg of total RNA was converted to cDNA using random primers (Takara, Otsu, Japan) with SuperScript II RNaseH- reverse transcriptase (Gibco BRL, Rockville, MD, USA). Those cDNAs were at first amplified with *GAPDH* primers for 27 cycles and the amounts of the PCR products were measured by ALF Express™ sequencer and normalized. The amplification was performed 35 or 40 cycles of 95°C for 30 s, 57 or 59 or 61°C for 15 s and 72°C for 60 s, and the final extension was at 72°C for 5 min, using a Perkin-Elmer Thermalcycler 9700 (Perkin-Elmer, Foster City, CA, USA). The PCR products

were run on 2% agarose gels and stained with ethidium bromide. We defined the gene as differentially expressed when it exhibits differential expression between the tumor and its corresponding normal liver in more than four out of the eight samples.

Northern blot analysis

In all, 25 μg of total RNA from the primary HBLs, HCC, and their corresponding normal livers were subjected to Northern analysis. Total RNA was prepared according to the method of Chomczynski and Sacchi (1987). Total RNA was fractionated by electrophoresis on 1% agarose gel containing formaldehyde, transferred onto a nylon membrane filter, and immobilized by UV crosslinking. The hybridization cDNA probe was a 976-base pair human *PLK1* cDNA fragment and labeled with [α-^{32}P]-dCTP using the BcaBEST random priming kit (Takara Biomedicals). The filter was hybridized at 65°C in a solution containing 1 M NaCl, 1% SDS, 7.5% dextran sulfate, 100 μg/ml of heat-denatured salmon sperm DNA, and radiolabeled probe DNA.

Quantitative real-time RT–PCR of PLK1

The primer set for amplification of the *PLK1* and probe sequence are as follows: forward primer, 5′-GCTGCACAAG AGGAGGAAA-3′; reverse primer, 5′-AGCTTGAGGTCTC-GATGAATAAC-3′; probe, 5′-CCTGACTGAGCCTGAGG CCCGATAC-TA-3′. Taqman *GAPDH* control reagents (Perkin-Elmer/Applied Biosystems) were used for the amplification of *GAPDH* as recommended by the manufacturer. PCR was performed using ABI Prism 7700 Sequence Detection System (Perkin-Elmer/Applied Biosystems). In all, 2 μl of cDNA was amplified in a final volume of 25 μl containing 1 × Taqman PCR reaction buffer, 200 μM each dNTP, 0.9 μM each primer, and 200 nM Taqman probe. The optional thermal cycling condition was as follows: 40 cycles of a two-step PCR (95°C for 15 s, 60°C for 60 s) after the initial denaturation (95°C for 10 min). Experiments were carried out in triplicate for each data point.

Statistical analysis

Statistical analyses were performed using Mann–Whitney's *U*-test and Cox regression. A *P*-value of less than 0.05 was considered significant.

Acknowledgements
We are grateful to Shigeru Sakiyama and Toshinori Ozaki for critical reading of the manuscript, and Yoko Nakamura and Aiko Morohashi for experimental support. We thank Eriko Isogai, Naoko Sugimitsu, and Yuki Nakamura for preparing RNA and sequencing analysis, and Natsue Kitabayashi, Emiko Kojima, Emi Goto, and Hisae Murakami for technical assistance. We also thank the hospitals and institutions collaborating with the Japanese Study Group for Pediatric Liver Tumor (JPLT) for providing surgical specimens. This work was supported in part by the fund from Hisamitsu Pharmaceutical Company and a grant-in-aid for Scientific Research on Priority Areas (C) 'Medical Genome Science' from the Ministry of Education, Culture, Sports, Science, and Technology of Japan.

References

Albrecht S, Von Schweinitz D, Waha A, Kraus JA, Von Deimling A and Pietsch T. (1994). *Cancer Res.*, **54**, 5041–5044.
Brady RO, Filling-Katz MR, Barton NW and Pentchev PG. (1989). *Neurol. Clin.*, **7**, 75–88.
Buendia MA. (1992). *Adv. Cancer Res.*, **59**, 167–226.
Buendia MA. (2002). *Med. Pediatr. Oncol.*, **39**, 530–535.
Chomczynski P and Sacchi N. (1987). *Anal. Biochem.*, **162**, 156–159.
Clay FJ, McEwen SJ, Bertoncello I, Wilks AF and Dunn AR. (1993). *Proc. Natl. Acad. Sci. USA*, **90**, 4882–4886.
Dietzmann K, Kirches E, Von Bossanyi, Jachau K and Mawrin C. (2001). *J. Neurooncol.*, **53**, 1–11.
Exelby PR, Filler RM and Grosfeld JL. (1975). *J. Pediatr. Surg.*, **10**, 329–337.
Fukuzawa R, Umezawa A, Ochi K, Urano F, Ikeda H and Hata J. (1999). *Int. J. Cancer*, **82**, 490–497.
Giardiello FM, Petersen GM, Brensinger JD, Luce MC, Cayouette MC, Bacon J, Booker SV and Hamilton SR. (1996). *Gut*, **39**, 867–869.
Glover DM, Ohkura H and Tavares A. (1996). *J. Cell Biol.*, **135**, 1681–1684.
Goldstein JL and Brown MS. (1990). *Nature*, **343**, 425–430.
Gray SG, Eriksson T, Ekstrom C, Holm S, Von Schweinitz D, Kogner P, Sandstedt B, Pietsch T and Ekstrom TJ. (2000). *Br. J. Cancer*, **82**, 1561–1567.
Haas JE, Muczynski KA, Krailo M, Ablin A, Land V, Vietti TJ and Hammond GD. (1989). *Cancer*, **64**, 1082–1095.
Hamanaka R, Kohno K, Seguchi T, Okamura K, Morimoto A, Ono M, Ogata J and Kuwano M. (1992). *J. Biol. Chem.*, **267**, 13160–13165.
Hata Y. (1990). *Jpn. J. Surg.*, **20**, 498–502.
Hata Y, Ishizu H, Ohmori K, Hamada H, Sasaki F, Uchino J, Inoue K, Naitoh H, Fujita M, Kobayashi T and Yokoyama S. (1991). *Cancer*, **68**, 2566–2570.
Hsieh JC, Kodjabachian L, Rebbert ML, Rattner A, Smallwood PM, Samos CH, Nusse R, Dawid IB and Nathans J. (1999). *Nature*, **398**, 431–436.
Ichimiya S, Nimura Y, Kageyama H, Takada N, Sunahara M, Shishikura T, Nakamura Y, Sakiyama S, Seki N, Ohira M, Kaneko Y, McKeon F, Caput D and Nakagawara A. (1999). *Oncogene*, **18**, 1061–1066.
Idilman R, De Maria N, Colantoni A and Van Thiel DH. (1998). *J. Viral. Hepat.*, **5**, 285–299.
Kinoshita M and Miyata M. (2002). *Hepatology*, **36**, 433–438.
Kinzler KW and Vogelstein B. (1996). *Cell*, **87**, 159–170.
Knecht R, Elez R, Oechler M, Solbach C, Von Ilberg C and Strebhardt K. (1999). *Cancer Res.*, **59**, 2794–2797.
Koch A, Denkhaus D, Albrecht S, Leuschner I, Von Schweinitz D and Pietsch T. (1999). *Cancer Res.*, **59**, 269–273.
Kotani S, Tugendreich S, Fujii M, Jorgensen PM, Watanabe N, Hoog C, Hieter P and Todokoro K. (1998). *Mol. Cell*, **1**, 371–380.
Lane HA and Nigg EA. (1996). *J. Cell Biol.*, **135**, 1701–1713.
Li FP, Wendy AT, Seddon J and Holmes GE. (1987). *J. Am. Med. Assoc.*, **257**, 2475–2477.
Li X, Adam G, Cui H, Sandstedt B, Ohlsson R and Ekstrom TJ. (1995). *Oncogene*, **11**, 221–229.
Liu X and Erikson RL. (2003). *Proc. Natl. Acad. Sci. USA*, **100**, 5789–5794.

Loftus SK, Morris JA, Carstea ED, Gu JZ, Cummings C, Brown A, Ellison J, Ohno K, Rosenfeld A, Tagle DA, Pentchev PG and Pavan WJ. (1997). *Science*, **277**, 232–235.
Mann JR, Lakin GE, Leonard JC, Rawlinson HA, Richardson SG, Corkery JJ, Cameron AH and Shah KJ. (1978). *Arch. Dis. Child*, **53**, 366–374.
Miao J, Kusafuka T, Udatsu Y and Okada A. (2003). *Hepatol. Res.*, **25**, 174–179.
Montagna M, Menin C, Chieco-Bianchi L and D'Andrea E. (1994). *J. Cancer Res. Clin. Oncol.*, **120**, 732–736.
Morin PJ, Sparks AB, Korinek V, Barker N, Clevers H, Vogelstein B and Kinzler KW. (1997). *Science*, **275**, 1787–1790.
Nagata T, Takahashi Y, Ishii Y, Asai S, Nishida Y, Murata A, Koshinaga T, Fukuzawa M, Hamazaki M, Asami K, Ito E, Ikeda H, Takamatsu H, Koike K, Kikuta A, Kuroiwa M, Watanabe A, Kosaka Y, Fujita H, Miyake M and Mugishima H. (2003). *Cancer Genet. Cytogenet.*, **145**, 152–160.
Nigg EA. (1998). *Curr. Opin. Cell Biol.*, **10**, 776–783.
Oda H, Nakatsuru Y, Imai Y, Sugimura H and Ishikawa T. (1995). *Int. J. Cancer*, **60**, 786–790.
Oda H, Imai Y, Nakatsuru Y, Hata J and Ishikawa T. (1996). *Cancer Res.*, **56**, 3320–3323.
Okabe H, Satoh S, Kato T, Kitahara O, Yanagawa R, Yamaoka Y, Tsunoda T, Furukawa Y and Nakamura Y. (2001). *Cancer Res.*, **61**, 2129–2137.
Okubo K, Hori N, Matoba R, Niiyama T, Fukushima A, Kojima Y and Matsubara K. (1992). *Nat. Genet.*, **2**, 173–179.
Ortega JA, Krailo MD, Haas JE, King DR, Ablin AR, Quinn JJ, Feusner J, Campbell JR, Lloyd DA, Cherlow J and Hammond GD. (1991). *J. Clin. Oncol.*, **9**, 2167–2176.
Park WS, Oh RR, Park JY, Kim PJ, Shin MS, Lee JH, Kim HS, Lee SH, Kim SY, Park YG, An WG, Kim HS, Jang JJ, Yoo NJ and Lee JY. (2001). *J. Pathol.*, **193**, 483–490.
Polakis P. (1999). *Curr. Opin. Genet. Dev.*, **9**, 15–21.
Qian YW, Erikson E, Li C and Maller JL. (1998). *Mol. Cell. Biol.*, **18**, 4262–4271.
Rainier S, Dobry CJ and Feinberg AP. (1995). *Cancer Res.*, **55**, 1836–1838.
Ribbeck K, Lipowsky G, Kent HM, Stewart M and Gorlich D. (1998). *EMBO J.*, **17**, 6587–6598.
Rimm DL, Caca K, Hu G, Harrison FB and Fearon ER. (1999). *Am. J. Pathol.*, **154**, 325–329.
Ryazanov AG, Pavur KS and Dorovkov MV. (1999). *Curr. Biol.*, **9**, R43–45.
Sasaki F, Matsunaga T, Iwafuchi M, Hayashi Y, Ohkawa H, Ohira M, Okamatsu T, Sugito T, Tsuchida Y, Toyosaka A, Nagahara N, Nishihira H, Hata Y, Uchino J, Misugi K and Ohnuma N. (2002). *J Pediatr Surg.*, **37**, 851–856.
Smith MR, Wilson ML, Hamanaka R, Chase D, Kung H, Longo DL and Ferris DK. (1997). *Biochem. Biophys. Res. Commun.*, **234**, 397–405.
Sudhof TC, Russell DW, Brown MS and Goldstein JL. (1987). *Cell*, **48**, 1061–1069.
Suzuki Y, Yoshitomo-Nakagawa K, Maruyama K, Suyama A and Sugano S. (1997). *Gene*, **200**, 149–156.
Takai N, Miyazaki T, Fujisawa K, Nasu K, Hamanaka R and Miyakawa I. (2001). *Cancer Lett.*, **164**, 41–49.
Takayasu H, Horie H, Hiyama E, Matsunaga T, Hayashi Y, Watanabe Y, Suita S, Kaneko M, Sasaki F, Hashizume K, Ozaki T, Furuuchi K, Tada M, Ohnuma N and Nakagawara A. (2001). *Clin. Cancer Res.*, **7**, 901–908.
Taniguchi K, Roberts LR, Aderca IN, Dong X, Qian C, Murphy LM, Nagorney DM, Burgart LJ, Roche PC, Smith DI, Ross JA and Liu W. (2002). *Oncogene*, **21**, 4863–4871.
Thomas D, Pritchard J, Davidson R, McKiernan P, Grundy RG and de Ville de Goyet J. (2003). *Eur. J. Cancer*, **39**, 2200–2204.
Tokumitsu Y, Mori M, Tanaka S, Akazawa K, Nakano S and Niho Y. (1999). *Int. J. Oncol.*, **15**, 687–692.
Toyoshima-Morimoto F, Taniguchi E, Shinya N, Iwamatsu A and Nishida E. (2001). *Nature*, **410**, 215–220.
Uotani H, Yamashita Y, Masuko Y, Shimoda M, Murakami A, Sakamoto T, Tazawa K and Tsukada K. (1998). *J. Pediatr. Surg.*, **33**, 639–641.
Van Tornout JM, Buckley JD, Quinn JJ, Feusner JH, Krailo MD, King DR, Hammond GD and Ortega JA. (1997). *J. Clin. Oncol.*, **15**, 1190–1197.
Velculescu VE, Vogelstein B and Kinzler KW. (2000). *Trends Genet.*, **16**, 423–425.
Von Horn H, Tally M, Hall K, Eriksson T, Ekstrom TJ and Gray SG. (2001). *Cancer Lett.*, **162**, 253–260.
Von Schweinitz D, Hecker H, Harms D, Bode U, Weinel P, Burger D, Erttmann R and Mildenberger H. (1995). *J. Pediatr. Surg.*, **30**, 845–852.
Von Schweinitz D, Wischmeyer P, Leuschner I, Schmidt D, Wittekind C, Harms D and Mildenberger H. (1994). *Eur. J. Cancer*, **30A**, 1052–1058.
Wang J, Shou J and Chen X. (2000). *Oncogene*, **19**, 1843–1848.
Weber RG, Pietsch T, Von Schweinitz D and Lichter P. (2000). *Am. J. Pathol.*, **157**, 571–578.
Wei Y, Fabre M, Branchereau S, Gauthier F, Perilongo G and Buendia MA. (2000). *Oncogene*, **19**, 498–504.
Weinberg AG and Finegold M. (1983). *Hum. Pathol.*, **14**, 512–537.
Wissmann C, Wild PJ, Kaiser S, Roepcke S, Stoehr R, Woenckhaus M, Kristiansen G, Hsieh JC, Hartmann A, Knuechel R, Rosenthal A and Pilarsky C. (2003). *J. Pathol.*, **201**, 204–212.
Wolf G, Elez R, Doermer A, Holtrich U, Ackermann H, Stutte HJ, Altmannsberger HM, Rubsamen-Waigmann H and Strebhardt K. (1997). *Oncogene*, **14**, 543–549.
Xu XR, Huang J, Xu ZG, Qian BZ, Zhu ZD, Yan Q, Cai T, Zhang X, Xiao HS, Qu J, Liu F, Huang QH, Cheng ZH, Li NG, Du JJ, Hu W, Shen KT, Lu G, Fu G, Zhong M, Xu SH, Gu WY, Huang W, Zhao XT, Hu GX, Gu JR, Chen Z and Han ZG. (2001). *Proc. Natl. Acad. Sci. USA*, **98**, 15089–15094.
Yun K, Jinno Y, Sohda T, Niikawa N and Ikeda T. (1998). *J. Pathol.*, **185**, 91–98.

Int. J. Cancer: **112**, 365–375 (2004)

Publication of the International Union Against Cancer

LOW EXPRESSION OF HUMAN TUBULIN TYROSINE LIGASE AND SUPPRESSED TUBULIN TYROSINATION/DETYROSINATION CYCLE ARE ASSOCIATED WITH IMPAIRED NEURONAL DIFFERENTIATION IN NEUROBLASTOMAS WITH POOR PROGNOSIS

Chiaki KATO[1,2], Kou MIYAZAKI[1], Atsuko NAKAGAWA[3], Miki OHIRA[1], Yohko NAKAMURA[1], Toshinori OZAKI[1], Toshio IMAI[2] and Akira NAKAGAWARA[1]*

[1]*Division of Biochemistry, Chiba Cancer Center Research Institute, Chiba, Japan*
[2]*Department of Physiologic Chemistry Faculty of Science, Toho University, Chiba, Japan*
[3]*Second Department of Pathology, Aichi Medical University, Nagakute, Japan*

Neuroblastoma (NBL), one of the most common childhood solid tumors, has a distinct nature in different prognostic subgroups. However, the precise mechanism underlying this phenomenon remains largely unknown. To understand the molecular and genetic bases of neuroblastoma, we have generated its cDNA libraries and identified a human ortholog of *tubulin tyrosine ligase* gene (*hTTL/Nbla0660*) as a differentially expressed gene at high levels in a favorable subset of the tumor. Tubulin is subjected to several types of evolutionarily conserved posttranslational modification, including tyrosination and detyrosination. Tubulin tyrosine ligase catalyzes ligation of the tyrosine residue to the COOH terminus of the detyrosinated form of α-tubulin. The measurement of *hTTL* mRNA expression in 74 primary neuroblastomas by quantitative real-time reverse transcription-PCR revealed that its high expression was significantly associated with favorable stages (1, 2 and 4s; $p = 0.0069$), high *TrkA* expression ($p = 0.002$), a single copy of *MYCN* ($p < 0.00005$), tumors found by mass screening ($p = 0.0042$), nonadrenal origin ($p = 0.0042$) and good prognosis ($p = 0.023$). The log-rank test showed that high expression of *hTTL* was an indicator of favorable prognosis ($p = 0.026$). Immunohistochemical analysis using specific antibodies generated by us demonstrated that tyrosinated tubulin (Tyr-tubulin), detyrosinated tubulin (Glu-tubulin) and hTTL as well as Δ2-tubulin were positive in favorable tumors, whereas only Δ2-tubulin was positive in the tumors with *MYCN* amplification. In an RTBM1 neuroblastoma cell line, hTTL was increased after treating the cells with bone morphogenetic protein 2 (BMP2) or all-trans retinoic acid (RA), which induced neuronal differentiation. These results suggest that the deregulated tubulin tyrosination/detyrosination cycle caused by decreased expression of hTTL is associated with inhibition of neuronal differentiation and enhancement of cell growth in the primary neuroblastomas with poor outcome.

Key words: *tubulin tyrosine ligase; tubulin tyrosination; neuroblastoma; neuronal differentiation; prognostic factor*

Tubulin is one of the most important molecular components that regulate cytoskeletal structure relating to cell motility, cell division, differentiation, invasion and metastasis in cancer. However, functional modification of tubulin protein has still been elusive. Tubulin is subjected to several types of evolutionarily conserved posttranslational modification that includes tyrosination/detyrosination, acetylation, phosophorylation, palmitoylation, polyglutamylation and polyglycylation.[1–4] The discovery of tyrosination cycle stems from the serial observations that the addition of radiolabeled tyrosine to a rat brain cytosolic extract leads to tyrosination of the COOH terminus of a single endogenous protein, α-tubulin, by a translation-independent mechanism.[5–7] Posttranslational incorporation of tyrosine into the tubulin has also been shown to occur *in vivo*.[8–10] The cycle of tyrosination/detyrosination is evolutionarily conserved[11–13] and is regulated by both tubulin tyrosine ligase (TTL) and carboxypeptidase, the gene of which has not yet been identified (Fig. 1). Microtubule dynamics is also an important factor. TTL protein was first purified by immunoaffinity chromatography from the lysates of bovine and porcine brains and was extensively characterized by protein sequencing.[14] Recently, rat *TTL* cDNA has also been isolated.[15] Interestingly, in 1991, Paturle-Lafanechere *et al.*[16] identified a nontyrosinatable variant of tubulin that lacked 2 amino acid residues, glutamic acid and tyrosine, at the COOH terminus (Δ2-tubulin). Δ2-tubulin was found to accumulate in mature neurons and in stable microtubule assemblies in cells.[17,18] In some tumors, it also accumulated in the cellular cytoplasm in association with decreased levels of TTL, suggesting that the amount of Δ2-tubulin and TTL expression level in tumor cells are important to define the malignant grade of cancer.[19] However, pathophysiologic significance of the tyrosination/detyrosination cycle in normal and cancer cells still remains unclear.

Neuroblastoma (NBL) is one of the most common childhood solid tumors and has distinct biologic characteristics in different prognostic subgroups. For example, NBL in patients under 1 year of age usually regresses spontaneously, whereas that in patients over 1 year of age often grows aggressively and eventually kills the patient. To understand the molecular mechanism of distinct biology and tumorigenesis of NBL, we have previously performed a comprehensive approach to unveil the gene expression profiles among the NBL subsets.[20,21] We constructed the subset-specific oligo-capping cDNA libraries from the primary NBL tissues with favorable (stage 1, high expression of *TrkA* and a single copy of *MYCN*) and unfavorable (stage 3 or 4, decreased expression of *TrkA* and *MYCN* amplification) characteristics and randomly cloned 4,654 cDNAs. After adding the cDNAs obtained from the stage 4s NBL cDNA library to our NBL gene collection, we made an in-house cDNA microarray carrying 5,340 genes proper to NBL. The comprehensive analysis of 136 NBLs using the microar-

Abbreviations: BMP2, bone morphogenetic protein 2; DMEM, Dulbecco's modified Eagle's medium; ECL, enhanced chemiluminescence; FBS, fetal bovine serum; hTTL, human tubulin tyrosine ligase; NBL, neuroblastoma; RA, retinoic acid; TCP, tubulin carboxypeptidase; TTL, tubulin tyrosine ligase.

Grant sponsor: Grant-in-Aid for Scientific Research and for Scientific Research on Priority Areas, Medical Genome Science from the Ministry of Education, Science, Sports and Culture, Japan; Grant sponsor: Hisamitsu Pharmaceutical Co. Inc.

*Correspondence to: Division of Biochemistry, Chiba Cancer Center Research Institute, 666-2 Nitona, Chuoh-ku, Chiba 260-8717, Japan. Fax: +81-43-265-4459. E-mail: akiranak@chiba-ccri.chuo.chiba.jp

Received 27 January 2004; Accepted 15 April 2004

DOI 10.1002/ijc.20431
Published online 23 June 2004 in Wiley InterScience (www.interscience.wiley.com).

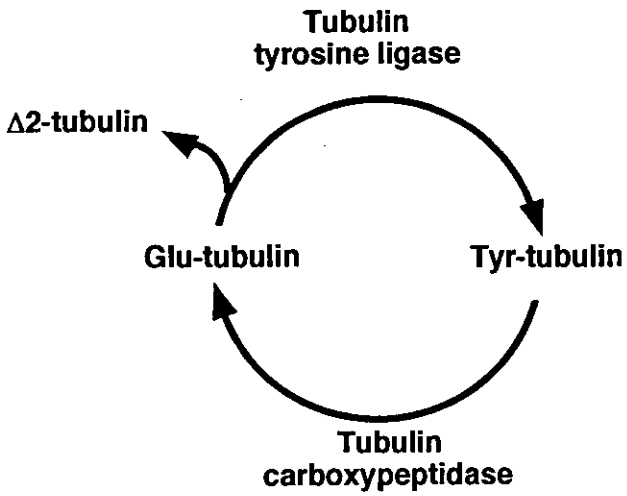

FIGURE 1 – The tyrosination/detyrosination cycle catalyzed by tubulin tyrosine ligase and tubulin carboxypeptidase.

ray showed that many genes that are related to the cytoskeletal components, including α-tubulin, had prognostic significance (data not shown).

In the present study, we have cloned for the first time the human ortholog of TTL (*hTTL*) from both the NBL and a fetal brain cDNA libraries. The analysis using 74 primary NBLs shows that expression of *hTTL* mRNA is significantly lower in unfavorable NBLs than in favorable tumors. The examination using specific antibodies raised against hTTL, Tyr-tubulin, Glu-tubulin and Δ2-tubulin demonstrates that hTTL is increased during induction of neuronal differentiation of cultured NBL cells treated with BMP2 or RA. The immunohistochemical study shows that hTTL, Tyr-tubulin, Glu-tubulin and Δ2-tubulin are positive in favorable NBLs, whereas only Δ2-tubulin is positive in aggressive NBLs with *MYCN* amplification. These suggested that the tyrosination/detyrosination cycle of α-tubulin is active in NBLs with high potential to differentiate or undergo apoptosis, while it is disregulated by downregulation of hTTL in *MYCN*-amplified NBLs, resulting in accumulation of Δ2-tubulin.

MATERIAL AND METHODS

Tumor specimen

Fresh frozen tumor tissues obtained by surgery or biopsy were sent to the Division of Biochemistry, Chiba Cancer Center Research Institute, from various hospitals in Japan with informed consent. Ninety tumors examined in this study were staged according to the International Neuroblastoma Staging System (INSS).[22] The number of tumors subjected to quantitative real-time RT-PCR were 24 in stage 1, 11 in stage 2, 5 in stage 4s, 10 in stage 3 and 24 in stage 4. The patients were treated according to the protocols previously described.[23] Biologic information on each tumor, including *MYCN* gene copy number, *TrkA* gene expression and DNA ploidy, was analyzed in our laboratory as described previously.[24]

Cell culture and transfection

COS7 and HEK293T cells were maintained in Dulbecco's modified Eagle's medium (DMEM) supplemented with 10% heat-inactivated fetal bovine serum (FBS; Life Technologies, Gaithersburg, MD) and penicillin (100 IU/ml)/streptomycin (100 μg/ml). Human neuroblastoma RTBM1 cells were grown in RPMI-1640 medium containing 10% heat-inactivated FBS and antibiotic mixture. Cultures were maintained at 37°C in a water-saturated atmosphere of 5% CO_2 in air. Transient transfection was performed by LipofectAMINE 2000 transfection reagent (Invitrogen, Carlsbad, CA) according to the manufacturer's instructions. In brief, cells were seeded in tissue culture plates to achieve 50% confluence. Twenty-four hours later, cells were transfected by using a mixture of the expression plasmids and LipofectAMINE 2000 transfection reagent in DMEM without serum. Forty-eight hours after transfection, cells were collected and analyzed by Western blotting. For neurite extension assays, RTBM1 cells were treated either with recombinant human BMP2 (Yamanouchi Pharmaceutical, Tokyo, Japan) or with RA at a final concentration of 1 nM or 5 μM, respectively.

RNA isolation and semiquantitative RT-PCR

Total RNA was prepared from neuroblastoma tissues according to the AGPC method.[25] Five micrograms of total RNA were subjected to the synthesis of the first-strand cDNA with $pd(N)_6$ random hexamer (Takara Shuzo, Otsu, Japan) and a Superscript II reverse transcriptase (Invitrogen) at 42°C for 90 min. The resultant cDNA was diluted to be a 1:20 solution and was amplified in a final volume of 10 μl of reaction mixture containing 100 μM of each deoxynucleoside triphosphate, 1 × PCR buffer, 1 μM of each primer and 0.2 U of rTaq DNA polymerase (Takara Bio, Ohtsu, Japan). The following primers were used: *hTTL*, 5′-CAGCTCTTCGGCTTTGACTT-3′ (sense) and 5′-GCTGTGGGCTGGATAAAGAG-3′ (antisense); human *GAPDH*, 5′-ACCTGACCTGCCGTCTAGAA-3′ (sense) and 5′-TCC ACCACCCTGTTGCTGTA-3′ (antisense). PCR templates were standardized by its *GAPDH* expression before performing semiquantitative PCR experiment. The PCR-amplified products were separated by electrophoresis on a 1.5% agarose gel and visualized by ethidium bromide poststaining.

Quantitative real-time RT-PCR

cDNA was prepared by the same method as in the semiquantitative RT-PCR and 2 μl of the 40-fold dilution was used for each PCR reaction. Primers and TaqMan probes for *hTTL* were designed using the primer design software Primer Express (Perkin-Elmer Applied Biosystems, Foster City, CA). The primer sequences for *hTTL* are 5′-AAGGAACTGCCTCCTGAGC-3′ and 5′-TCAATGAGCCAC ACCTTCA-3′. The probe sequence for *TTL* is 5′-FAM-ATTAGC ACCAAGCACCTCCCTTACCAGAGC-TAMRA-3′. PCR was carried out with the ABI Prism 7700 Sequence Detection System (Perkin-Elmer Applied Biosystems). Two μl of cDNA was amplified in a final volume of 25 μl containing 1 × TaqMan mixture, 300 nM each primer and 200 nM TaqMan probe. The thermal cycling condition was as follows: 50 cycles of a 2-step PCR (95°C for 15 sec, 60°C for 1 min) after the initial activation of UNG followed by denaturation (50°C for 2 min, 95°C for 10 min). TaqMan *GAPDH* control reagent kit (Roche Molecular Biochemicals, Basel, Switzerland) was used for the amplification of *GAPDH* according to the manufacturer's instructions; all data were normalized using *GAPDH* expression. The experiments were performed in triplicate for each data point.

Generation of polyclonal anti-hTTL antibodies

The polyclonal anti-hTTL antibody was raised in rabbits against Cys-coupled synthetic peptides derived from hTTL (222-RTASEPY-HVDNFQDKTCHLTNH-243 and 244-CIQKEYSKNYGKYEE-GNE-261). The polyclonal anti-Tyr-tubulin, anti-Glu-tubulin and anti-Δ2-tubulin antibodies were raised in rabbits immunized with Cys-coupled synthetic peptides corresponding to their COOH termini (CEEEGEEY, CGEEEGEE and CEGEEEGE, respectively). Antibodies were purified by using peptide-coupled affinity columns and tested for their ability to identify the corresponding proteins by Western blots. The synthetic peptides and antibodies were generated by Protein Express (Chiba, Japan).

Construction of FLAG-tagged hTTL expression plasmid

The FLAG-tagged hTTL expression plasmid was generated by PCR amplification using the cDNA library derived from human fetal brain (Stratagene, La Jolla, CA) and an *hTTL* cDNA that lacked the 5′-portion encoding the NH_2 terminal region of hTTL as templates. The forward and reverse primers used were 5′-TAAATAGTCGACGATATCATGGACTACAAGGACGAC

GACGACAAGTACACCTTCGTGGTACGCGATGAGAACAGC AGCGTCTACGCCGAGGTCTCCCGGCTGCTCCTCGCCA-3′ (sequence encoding FLAG epitope tag is in boldface, and *Eco*RV recognition site is underlined) and 5′-TACATGTCGACGCGG CCGCTCACAGCTTGAT GAA-3′ (*Not*I restriction site is underlined). The resulting PCR product was gel-purified, digested with *Eco*RV and *Not*I, inserted into identical restriction sites of a mammalian expression plasmid pIRESpuro2 (Clontech Laboratories, Palo Alto, CA) and its nucleotide sequence was verified by automated dideoxy terminator cycle sequencing.

Western blot analysis

Cells were washed in ice-cold phosphate-buffered saline (PBS), collected by centrifugation and lysed in 1 × sample buffer. Equal amounts of whole-cell lysates were fractionated by SDS-polyacrylamide gel electrophoresis (SDS-PAGE), and electrophoretically transferred onto a polyvinylidene difluoride (PVDF) membrane filter (Immobilon-P; Millipore, Billerica, MA). The filter was then blocked with Tris-buffered saline (TBS) containing 5% nonfat dry milk at room temperature for 1 hr and subsequently incubated for 1 hr with the antibodies against hTTL, Tyr-tubulin, Glu-tubulin, Δ2-tubulin, α-tubulin (5H1; PharMingen, San Diego, CA) and actin (20-33; Sigma Chemical, St. Louis, MO). The filter was further incubated with horseradish peroxidase-conjugated mouse or rabbit IgG secondary antibody (Cell Signaling Technologies, Beverly, MA). Immunoreactivity was detected using the enhanced chemiluminescence system (ECL; Amersham Pharmacia Biotechnology, Uppsala, Sweden) according to the manufacturer's instructions. The films were exposed at multiple time points to ensure that the images were not saturated.

Immunohistochemistry

Immunohistochemical stainings with antibodies against hTTL (1:100), Tyr-tubulin (1:100), Glu-tubulin (1:100) and Δ2-tubulin (1:100) were performed on 10 human neuroblastoma tumors selected from the surgical pathology file at the Department of Pathology, Aichi Medical University, based on the results of histopathology evaluation[26] and *MYCN* status. Also performed were immunostainings with antibodies against TrkA (1:40, 763; Santa Cruz Biotechnology, Santa Cruz, CA), CD56 (1B6; Novocastra Laboratories, Peterborough, U.K.) and Ki-67 (1:200, MIB-1; Dako, Kyoto, Japan) on the same tumor tissues. All of those tumor samples were obtained prior to chemotherapy and irradiation therapy and included 6 favorable histology cases with nonamplified *MYCN* (FH&NA) and 4 unfavorable histology cases with amplified *MYCN* (UH&A). Among the neuroblastoma cases, tumors in the FH&NA subset were reported to be the most favorable biologically and clinically. In contrast, tumors in the UH&A subset are known to be the most aggressive with the poorest clinical outcome.[27] Four μm thick sections from the formalin-fixed and paraffin-embedded tissue samples were deparaffinized and microwaved for 3 × 5 min in Na-citrate buffer (pH 6.0) for antigen retrieval. The slides were first immersed in 0.3% hydrogen peroxide in methanol for 20 min and then in 10% normal goat serum for 30 min. The primary antibodies were then applied at 4°C overnight, followed by a standard staining procedure using the Vectastain ABC kit (Vector Laboratories, Burlingame, CA). Sections were counterstained with hematoxylin for light microscopic review and evaluation. hTTL, Tyr-tubulin, Glu-tubulin and Δ2-tubulin were always positively detected in the cytoplasm and neuritic processes of normal ganglion cells in the separate positive control sections as well as in the test sections as built-in control, whenever available. As for the negative controls of hTTL, Tyr-tubulin, Glu-tubulin, Δ2-tubulin and TrkA stainings, normal rabbit immunoglobulins (1:500 dilution, Vector Laboratories) were applied as the primary antibody. As for the negative controls of CD56 and Ki-67 stainings, we followed the staining procedure without the primary antibodies.

Statistical analysis

Student's *t*-tests were used to explore possible associations between *hTTL* expression and other factors, such as age. Since the values of the *hTTL* expression were skewed, a log transformation was used to achieve the normality when using *t*-test and Cox regression. The distinction between high and low levels of *hTTL* was based on the median value (low, *hTTL* < 95 e.u.; high, *hTTL* > 95 e.u.), regardless of tumor stage, *MYCN* copy number, or survival. Kaplan-Meier survival curves were calculated, and survival distributions were compared using the log-rank test. Cox regression models were used to explore associations between *hTTL* expression, age, *MYCN* amplification, mass screening, origin and survival. Statistical significance was declared if the *p*-value was < 0.05. Statistical analysis was performed using Stata 7.0. (Stata, College Station, TX).

RESULTS

Cloning and expression of hTTL *gene*

We have previously constructed oligo-capping cDNA libraries from 3 fresh human NBL tissues (stages 1 and 2, high *TrkA* expression and a single copy of *MYCN*), which were gradually undergoing spontaneous regression probably due to neuronal apoptosis.[20] Screening of 1,152 novel genes by reverse transcriptase (RT)-PCR revealed that 194 genes were expressed differentially between NBLs with favorable prognosis and those with unfavorable outcome. Among them, we detected a partial cDNA sequence (*Nbla00660*) corresponding to the human ortholog of *tubulin tyrosine ligase* (*hTTL*) gene. We then cloned the full-length *hTTL* cDNA using both conventional phage library screening and genome sequence-based RT-PCR procedure. The *hTTL* gene was mapped to chromosome 2q13 and consisted of 7 exons (Fig. 2*a*) with 377 predicted amino acids (Genbank/DDBJ accession number AB071393; Fig. 2*b*). Comparison of the deduced amino acid sequence of human *TTL* cDNA with those of mouse, rat, pig and cow showed identity by 94%, 94%, 93% and 94%, respectively. *hTTL* was ubiquitously expressed in various human tissues including heart, kidney, lung, colon, thymus, spleen, mammary gland, testis, prostate, brain, cerebellum, liver, fetal brain, fetal liver, adrenal gland and skeletal muscle (Fig. 2*c*). However, it was rather preferentially expressed in adult and fetal brains and lung.

Specific antibodies and catalytic activity of hTTL

To study the role of hTTL and the tyrosination/detyrosination cycle regulated by TTL in neuroblastoma, we generated specific antibodies against human Tyr-tubulin, Glu-tubulin and Δ2-tubulin based on the previous reports.[16,18,28] The PVDF membranes spotted with equal amount (1 μg) of synthetic peptides corresponding to COOH terminal 7 amino acid residues of Tyr-tubulin (CEEEGEEY), Glu-tubulin (CGEEEGEE) and Δ2-tubulin (CEGEEEGE) were immunoblotted with rabbit anti-Tyr-tubulin antibody (Fig. 3*a*, top), anti-Glu-tubulin antibody (Fig. 3*a*, middle) and anti-Δ2-tubulin antibody (Fig. 3*a*, bottom), respectively. There were no crossreactivities among them, suggesting that those 3 antibodies were highly specific to each form of tubulin. To confirm the catalytic activity of hTTL encoded by the gene we cloned, we transfected the HEK293T cells with various amount of *hTTL* expression construct. Increased levels of hTTL in those cells induced tyrosination of tubulin in dose-dependent manner, while the level of endogenous Glu-tubulin was decreased (Fig. 3*c*). These results showed that hTTL protein encoded by the gene we cloned has its catalytic activity.

Upregulation of hTTL expression during neuronal differentiation

BMP2 has been characterized as a neurotrophic factor.[29] Recently, Nakamura *et al.*[30] have reported that RTBM1, a human neuroblastoma cell line, is responsive to both BMP2 and RA by extending neurites. By using this system, we examined whether the expression levels of hTTL change during induction of neuronal differentiation. As shown in Figure 4, the treatment of RTBM1

a

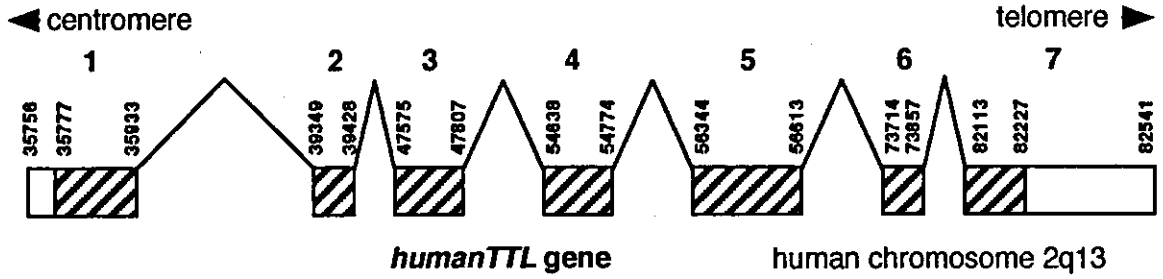

b

```
humanTTL  MYTFVVRDENSSVYAEVSRLLLATGHWKRLRRDNPRFNLMLGERNRLPFGRLGHEPGLVQLVNYYRGADKLCRKAS 76
mouseTTL  MYTFVVRDENSSVYAEVSRLLLATGYWKRLRRDNPRFNLMLGERNRLPFGRLGHEPGLAQLVNYYRGADKLCRKAS 76
ratTTL    MYTFVVRQENSSVYAEVSRLLLATGYWKRLRRDNPRFNLMLGGRNRLPFGRLGHEPGLAQLVNYYRGADKLCRKAS 76
pigTTL    MYTFVVRDENSSVYAEVSRLLLATGHWKRLRRDNPRFNLMLGERNRLPFGRLGHEPGLMQLVNYYRGADKLCRKAS 76
cowTTL    MYTFVVRDENSSVYAEVSRLLLATGHWKRLRRDNPRFNLMLGERNRLPFGRLGHEPGLMQLVNYYRGADKLCRKAS 76
          ******* ***************** ********** ********** ********** **********

humanTTL  LVKLIKTSPELAESCTWFPESYVIYPTNLKTPVAPAQNGIQPPISNSRTDEREFFLASYNRKKEDGEGNVWIAKSS 152
mouseTTL  LVKLVKTSPELSESCSWFPESYVIYPTNLKTPVAPAQNGIQLPVSNSRTDEREFFLASYNRKKEDGEGNVWIAKSS 152
ratTTL    LVKLVKTSPELSESCSWFPESYVIHPTNLKTPVAPAQNGIQLPVSNSRTDEREFFLASYNRKKEDGEGNVWIAKSS 152
pigTTL    LVKLIKTSPELAESCTWFPESYVIYPTNLKTPVAPAQNGIHPPIHSSRTDEREFFLTSYNKKKEDGEGNVWIAKSS 152
cowTTL    LVKLIKTSPELAESCTWFPESYVIYPTNLKTPVAPAQDGIHPPLHSSRTDEREFFLASYNRKKEEGEGNVWIAKSS 152
          **** ****** *** ******** ********** ** *  ********** *** *** **********

humanTTL  AGAKGEGILISSEASELLDFIDNQGQVHVIQKYLEHPLLLEPGHRKFDIRSWVLVDHQYNIYLYREGVLRTASEPY 228
mouseTTL  AGAKGEGILISSEASELLDFIDSQGQVHVIQKYLERPLLLEPGHRKFDIRSWVLVDHQYNIYLYREGVLRTASEPY 228
ratTTL    AGAKGEGILISSEASELLDFIDNQGQVHVIQKYLEHPLLLEPGHRKFDIRSWVLVDHQYNIYLYREGVLRTASEPY 228
pigTTL    AGAKGEGILISSEATELLDFIDNQGQVHVIQKYLERPLLLEPGHRKFDIRSWVLVDHQYNIYLYREGVLRTASEPY 228
cowTTL    AGAKGEGILISSDATELLDFIDNQGQVHVIQKYLERPLLLEPGHRKFDIRSWVLVDHQFNIYLYREGVLRTASEPY 228
          ********** * ******* ********** ********************** *****************

humanTTL  HVDNFQDKTCHLTNHCIQKEYSKNYGKYEEGNEMFFKEFNQYLTSALNITLESSILLQIKHIIRNCLLSVEPAIST 304
mouseTTL  HVDNFQDKTCHLTNHCIQKEYSKNYGKYEEGNEMFFEEFNQYLTSALNITLESSILLQIKHIIRSCLMSVEPAIST 304
ratTTL    HVDNFQDKTCHLTNHCIQKEYSKNYGKYEEGNEMFFEEFNQYLTSALNITLENSILLQIKHIIRSCLMSVEPAIST 304
pigTTL    HTDNFQDKTCHLTNHCIQKEYSKNYGKYEEGNEMFFEEFNQYLTSALNITLESSILLQIKHIIRSCLLSVEPAIST 304
cowTTL    HMDNFQDKTCHLTNHCIQKEYSKNYGKYEEGNEMFFEAFNRYLTSALNITLESSILLQIKHIIRSCLMSVEPAIST 304
          * ********************************** ** ********** ********** ** ********

humanTTL  KHLPYQSFQLFGFDFMVDEELKVWLIEVNGAPACAQKLYAELCQGIVDIAISSVFPPPPDVEQPQTQP--AAFIKL 377
mouseTTL  KHLPYQSFQLLGFDFMVDEELKVWLIEVNGAPACAQKLYAELCQGIVDIAISSVFPPPPDTEQVPQQP--AAFVKL 377
ratTTL    KHLPYQSFQLLGFDFMVDEELKVWLIEVNGAPACAQKLYAELCQGIVDIAISSVFPPPPDTEQVPQQP--AAFMKL 377
pigTTL    RHLPYQSFQLFGFDFMVDEDLKVWLIEVNGAPACAQKLYAELCQGIVDIAIASVFPPPPDAEQQQQQPPPAAFIKL 379
cowTTL    KHLPYQSFQLFGFDFMVDEELKVWLIEVNGAPACAQKLYAELCQGIVDIAIASVFPPPPDAEQQPPQP--ATFIKL 377
          ********* ******** ********************************** ******* **   **  * * **
```

c

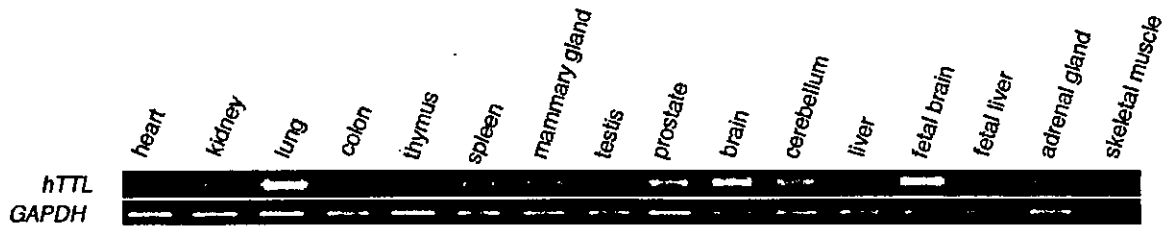

FIGURE 2

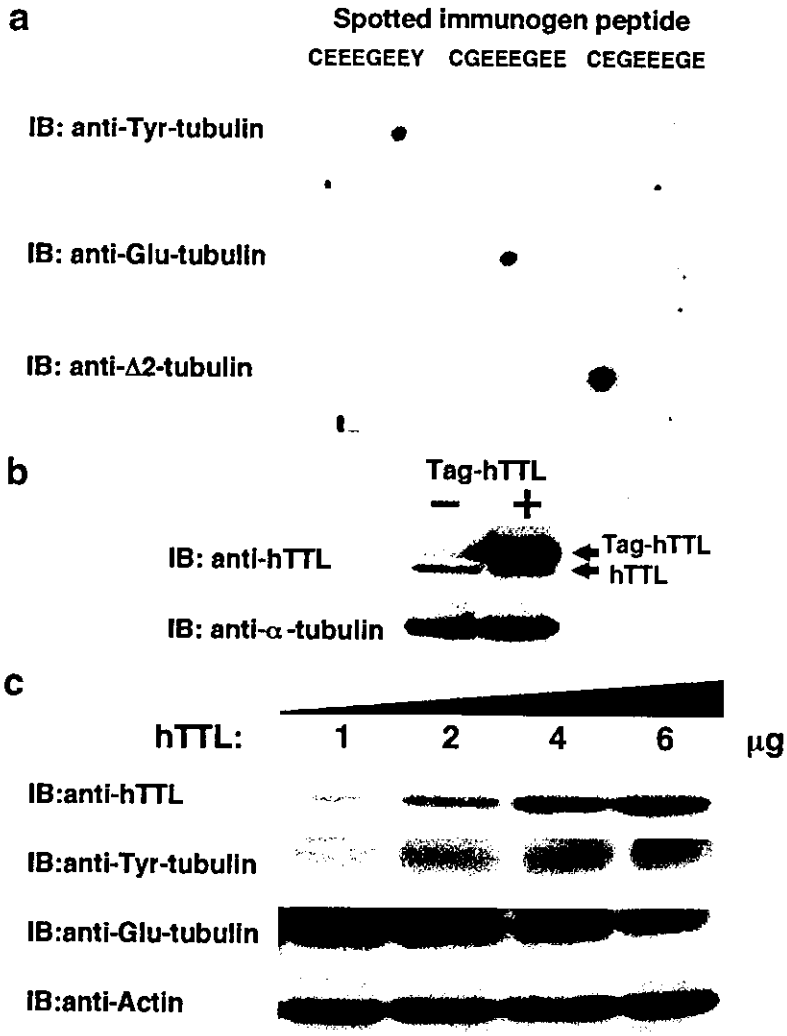

FIGURE 3 – hTTL has a tyrosination activity in mammalian cultured cells. (*a*) Specificity of antibodies. The indicated synthetic peptides were spotted on the filter and immunoblotted with the polyclonal anti-Tyr-tubulin (top), anti-Glu-tubulin (middle), or anti-Δ2-tubulin antibody (bottom). (*b*) Expression of FLAG-tagged hTTL. Whole-cell lysates prepared from COS7 cells transfected with the empty plasmid or with the expression plasmid for FLAG-tagged hTTL were subjected to immunoblotting with the anti-hTTL antibody (top). The expression level of α-tubulin was examined to ensure equal loading (bottom). (*c*) The exogenously expressed hTTL has a catalytic activity. HEK293T cells were transfected with increasing amounts of the hTTL expression plasmid. Forty-eight hours after transfection, whole-cell lysates were prepared and immunoblotted with the indicated antibodies. The expression level of actin is included as a loading control (bottom).

cells with 1 nM BMP2 or 5 μM RA induced remarkable morphologic differentiation by day 8. The hTTL protein level was increased after day 2 and peaked on day 6 in the former and on day 3 in the latter. Thereafter, it appeared to be decreased. Thus, hTTL was induced during induction of neuronal differentiation in NBL cells.

Expression of hTTL mRNA in primary neuroblastomas

To evaluate the clinical significance of *hTTL*, we examined the expression of *hTTL* mRNA in 16 favorable (stage 1, high expression of *TrkA* and a single copy of *MYCN*) and 16 unfavorable (stage 3 or 4, low expression of *TrkA* and amplification of *MYCN*) NBLs using semiquantitative RT-PCR. As shown in Figure 5(*a*), *hTTL* was preferentially expressed in favorable NBLs. Therefore, we next performed quantitative real-time RT-PCR to measure the levels of *hTTL* transcript in 74 primary NBLs. Table I shows the quantitative levels of *hTTL* mRNA expression (mean ± SEM) by age (< 1-year-old *vs.* ≥ 1-year-old), tumor stages (1 + 2 + 4s *vs.* 3 + 4), *TrkA* expression (low *vs.* high), *MYCN* gene copies (single *vs.* amplified), origin (adrenal gland *vs.* others), mass screening (tumors found by mass screening *vs.* sporadic tumors) and prognosis (alive *vs.* dead). High levels of *hTTL* expression were significantly associated with favorable stages ($p = 0.0069$), high *TrkA* expression ($p = 0.002$), a single copy of *MYCN* ($p < 0.00005$), tumors found by mass screening ($p = 0.0042$), origins other than adrenal gland ($p = 0.0042$) and a good prognosis ($p = 0.023$). *hTTL* expression was marginally associated with age. The log-rank test indicated that *hTTL* expression was associated with better survival ($p = 0.026$), which was also indicated in the Kaplan-Meier cumulative survival curves (Fig. 5*b*).

The univariate Cox regression was employed to examine the individual relationship of each variable to survival (Table II). Expression of *hTTL*, age, *MYCN* copy numbers and mass screening were found to be of prognostic importance, supporting the results of the log-rank test. However, since *hTTL* expression was highly associated with *MYCN*, mass screening and origin, multivariable Cox models were not fitted to assess the predictive importance of *hTTL* expression for survival after controlling these prognostic factors, suggesting that expression of *hTTL* was not an independent prognostic indicator.

FIGURE 2 – Genomic structure, alignment of amino acid sequence and mRNA expression of human *TTL*. (*a*) Genomic structure of *hTTL*. The *hTTL* gene that is mapped to 2q13 consists of 7 exons. Untranslated regions (open boxes) and coding regions (hatched boxes) are shown. Numbers indicate nucleotide position in human BAC clone *RP11-1124* (accession number AC012442). (*b*) Comparison of amino acid sequences among mammalian TTLs. The gaps produced by the alignment are indicated by a hyphen in the sequence. The conserved amino acid residues in TTLs are shown by asterisks below the alignment. (*c*) Tissue distribution of *hTTL* mRNA. The expression levels of *hTTL* mRNA in the indicated human tissues were examined by semiquantitative RT-PCR (top). *GAPDH* expression was also examined as an internal control (bottom).

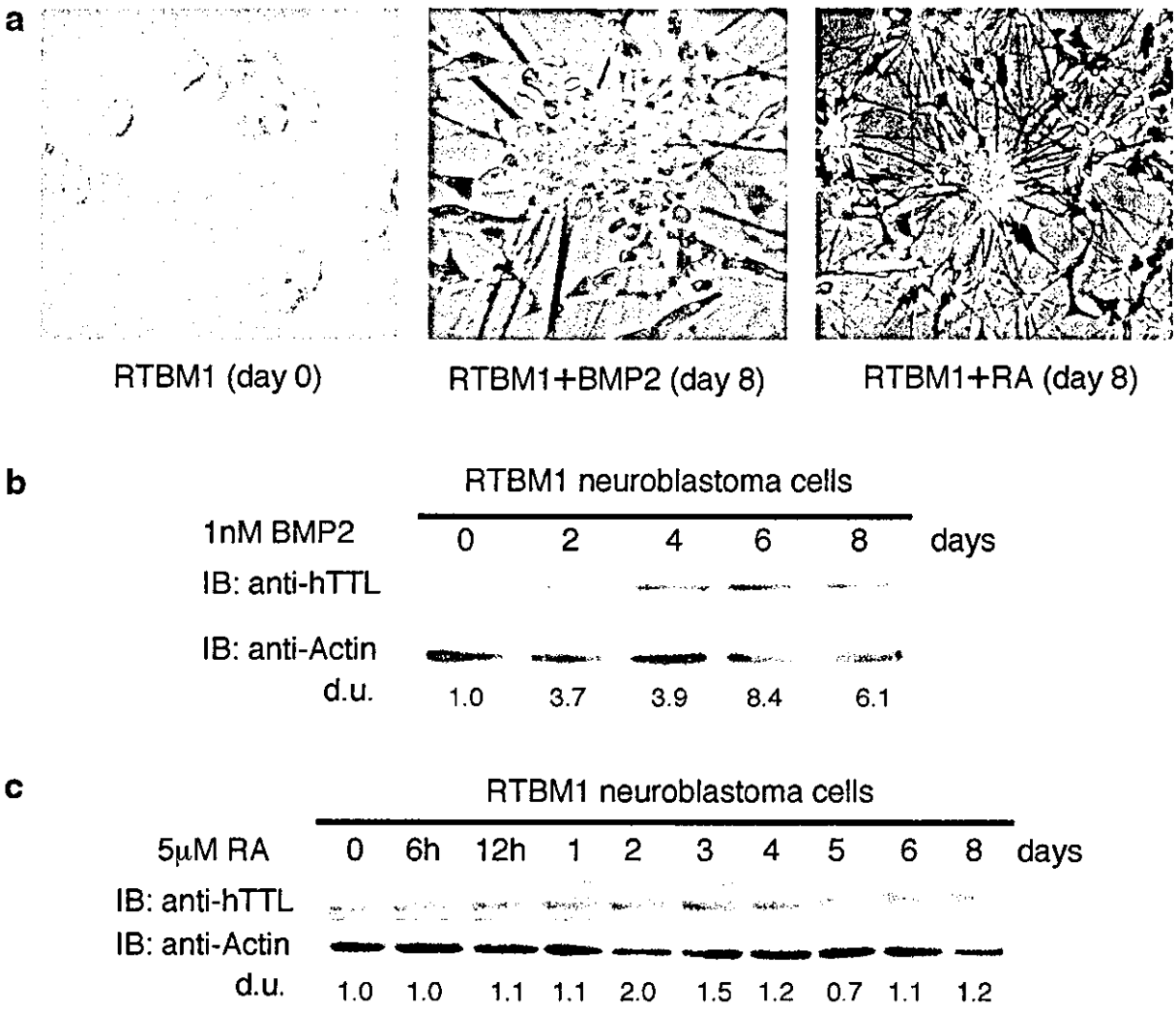

FIGURE 4 – TTL is induced during BMP2- and RA-mediated neuroblastoma differentiation. (*a*) BMP2- or RA-induced morphologic changes in RTBM1 neuroblastoma cells. RTBM1 cells were treated with BMP2 or RA at a final concentration of 1 nM or 5 μM, respectively, and maintained for 8 days. (*b*) Expression levels of hTTL are increased in response to BMP2. At the indicated time points after the treatment with BMP2 (at a final concentration of 1 nM), whole-cell lysates prepared from RTBM1 cells were subjected to immunoblotting with the antibody against hTTL (top). Actin protein levels were determined as a loading control (bottom). (*c*) Induction of hTTL in response to RA. RTBM1 cells were exposed to RA at a final concentration of 5 μM. Whole-cell lysates were prepared at the indicated time points after the treatment with RA and subjected to immunoblotting with the anti-hTTL (top) or with antiactin (bottom) antibody. d.u., arbitrary density units.

Immunohistochemistry

To determine the expression pattern of hTTL protein in primary NBLs, we performed immunohistochemical study for 6 favorable (stage 1 or 2 and a single copy of *MYCN*) and 4 unfavorable (stage 3 or 4 and amplified *MYCN*) NBLs. hTTL, Tyr-tubulin and Glu-tubulin were positively detected both in the cytoplasm of the neuroblastic cells and in the fine meshwork of neuropil of all 6 tumors with favorable histology (Shimada's classification) and a single copy of *MYCN* (Fig. 6*a–c*). In contrast, all 4 tumors with unfavorable histology and *MYCN* amplification were negative for Tyr-tubulin and Glu-tubulin, and only 1 tumor in this subset was positive for hTTL (Fig. 6*f–h*). Interestingly, all 10 NBL tumors were positive for Δ2-tubulin, but whose staining pattern was rather distinct in different subsets of the tumors. In the favorable tumors, Δ2-tubulin showed a localization similar to hTTL, Tyr-tubulin and Glu-tubulin and was detected in the cytoplasm and in the fine neuropil (Fig. 6*d*). On the other hand, Δ2-tubulin in the aggressive tumors was found only in the cytoplasm of neuroblastic cells, since they had no or a very limited capability of neuritic process production (*i.e.*, neuropil formation; Fig. 6*i*).

CD56 was detected in all 10 tumors, regardless of the histology and *MYCN* status (data not shown). TrkA was detected in all of 6 favorable tumors (Fig. 6*e*), but was negative in 3 of 4 aggressive tumors (Fig. 6*j*). It was noted that one unfavorable tumor with weakly positive trkA showed positive staining for TTL. Ki-67 staining revealed 10–20% and 60–70% positive cells in the favorable and the unfavorable tumors, respectively (data not shown).

DISCUSSION

In the present study, we have identified human ortholog of *tubulin tyrosine ligase* gene, which is highly conserved among the mammalian species. *hTTL* mRNA is ubiquitously expressed but rather preferential in both fetal and adult brains as well as in lung. The specific antibodies raised against hTTL, Tyr-tubulin, Glu-tubulin and Δ2-tubulin have confirmed the catalytic activity of

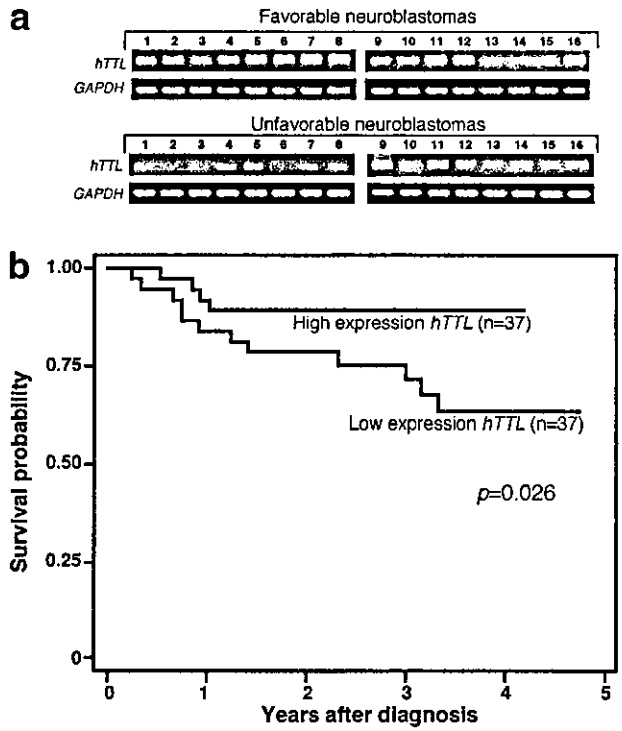

FIGURE 5 – Expression of *hTTL* mRNA is associated with unfavorable prognosis of neuroblastoma. (*a*) Total RNA was purified from the indicated favorable (top) and unfavorable NBL tissues (bottom) and subjected to semiquantitative RT-PCR. Sixteen favorable cases used in this study were classified as stage 1 NBL with a single copy *MYCN* as well as a high expression of *TrkA*. Sixteen unfavorable cases were in stages 3 and 4 NBL with *MYCN* amplification as well as a low *TrkA* expression. *GAPDH* expression was also examined as an internal control. (*b*) Association of *hTTL* mRNA expression levels with favorable prognosis of NBL. Total RNA was prepared from 74 NBL tissues, and *hTTL* mRNA levels were assayed by quantitative real-time RT-PCR as described in text. The values of *hTTL* mRNA were normalized by *GAPDH*. The survival of *hTTL* relatively high-expression group (n = 37) and *hTTL* low-expression group (n = 37) was compared using the Kaplan-Meier procedure.

TABLE I – RESULTS OF LOG-RANK TESTS FOR CONVENTIONAL PROGNOSTIC FACTORS AND EXPRESSION OF *hTTL* IN 74 PRIMARY NEUROBLASTOMAS

Variable	n	*hTTL* expression[1]	p-value
Age (year)			0.1
<1	43	117 ± 14	
≥1	31	77 ± 10	
Tumor stage			0.0069
1, 2, 4s	40	127 ± 14	
3, 4	34	69 ± 9	
TrkA expression			0.002
High	36	125 ± 17	
Low	38	77 ± 8	
MYCN			<0.00005
Single	52	123 ± 11	
Amplified	22	46 ± 9	
Mass screening			0.0042
+	37	128 ± 14	
−	37	72 ± 10	
Origin			0.0042
Adrenal gland	47	85 ± 11	
Others	27	127 ± 16	
Prognosis			0.023
Alive	58	113 ± 11	
Dead	16	54 ± 11	

[1]Mean ± SEM.

TABLE II – COX REGRESSION MODELS USING DICHOTOMOUS FACTORS OF AGE, *MYCN* AMPLIFICATION, MASS SCREENING, ORIGIN AND EXPRESSION OF *hTTL*

Factor	p-value	Hazard ratio (95% confidence interval)
hTTL expression (log)	0.024	0.64 (0.44, 0.94)
Age (> 1 *vs.* < 1 year)	0.005	5.04 (1.61, 15.8)
MYCN (1 copy *vs.* > 1 copy)	<0.0005	0.06 (0.017, 0.22)
Mass screening (+ *vs.* −)	0.004	0.05 (0.007, 0.38)
Origin (adrenal gland *vs.* others)	0.31	1.79 (0.58, 5.57)

hTTL encoded by the *hTTL* gene in the cells. Interestingly, hTTL is induced during neurite extension in RTBM1 NBL cells treated with BMP2 or RA, suggesting that hTTL expression is associated with neuronal differentiation in human NBL. Immunohistochemically, favorable NBLs are positive for hTTL, Tyr-tubulin, Glu-tubulin and Δ2-tubulin, whereas unfavorable tumors with *MYCN* amplification are positive only for Δ2-tubulin, suggesting that deregulation of tyrosination/detyrosination cycle contributes to malignant progression of NBL. This hypothesis has been further supported by a significant decrease of the levels of *hTTL* expression in the patients with poor prognosis.

The dynamics of microtubule regulates many cellular functions, including migration, motility, differentiation, cell division and cellular cap formation. Though posttranslational modifications of tubulin and their enzymatic regulation have long been studied, the precise mechanisms are still largely unknown. It is interesting that no orthologs of highly conserved mammalian TTL have so far been reported in *Caenorhabditis elegans*, *Drosophila melanogaster* and *Saccharomyces cerevisiae*, suggesting that the tyrosination/detyrosination cycle of tubulin may be related to evolution of the cellular functions, including neuronal differentiation. In newborn rats, TTL expression is found in skeletal muscle at high levels and is developmentally regulated by rapidly decreasing its level during early postnatal period.[31] It is interesting that both BMP2 and RA, which have increased levels of hTTL expression, function as regulators to induce differentiation during neural development.

The tyrosination/detyrosination of tubulin may be regulated by the activities of both TTL and tubulin carboxypeptidase (TCP). Until now, however, the *TCP* gene has never been identified in vertebrates, although biochemical TCP activity has been reported to be present in some subcellular fractions.[18] Tubulin is also posttranslationally modified by nitrotyrosination. Eiserich *et al.*[32] showed that free 3-nitrotyrosine (NO_2Tyr) is transported into mammalian cells and selectively incorporated into the Glu-tubulin posttranslationally, which is catalyzed by TTL. Cellular injury such as microtubule disorganization has consequently been induced. Kalisz *et al.*[33] also showed that nitrotyrosine can be incorporated into α-tubulin by *in vitro* assays. Those reports demonstrated that carboxypeptidase A is incapable of cleaving nitrotyrosine from the modified α-tubulin. On the other hand, Bisig *et al.*[34] reported that nitrotyrosinated tubulin is a good substrate of physiologic TCP, and that it has a similar capability to that of the tyrosinated tubulin to assemble into microtubules, suggesting that incorporation of nitrotyrosine is not injurious at least to dividing cells. Therefore, whether nitrotyrosinated tubulin is harmful or not is still controversial. Nevertheless, as increased nitrotyrosination is reported in Alzheimer's disease and amyotrophic lateral sclerosis,[35-37] the functional analysis of the role of hTTL and tubulin tyrosination/detyrosination cycle should be important for understanding the pathogenesis of these disease. The treatment of cells with methylmercury (MeHg) is also reported to induce perturbation of cellular activities associated with the tubulin/microtubule system by altering the status of tubulin tyrosination in the rat

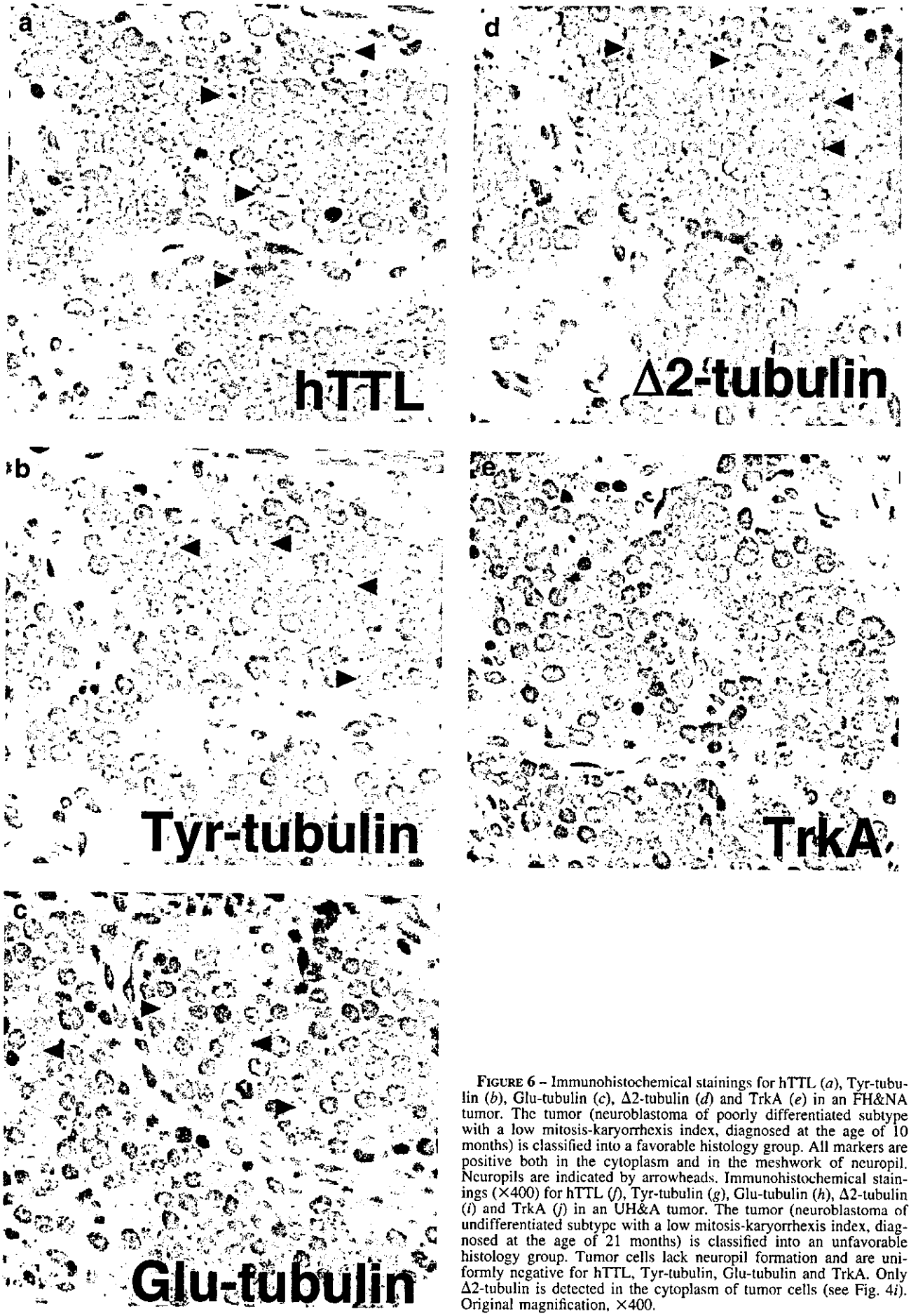

FIGURE 6 – Immunohistochemical stainings for hTTL (*a*), Tyr-tubulin (*b*), Glu-tubulin (*c*), Δ2-tubulin (*d*) and TrkA (*e*) in an FH&NA tumor. The tumor (neuroblastoma of poorly differentiated subtype with a low mitosis-karyorrhexis index, diagnosed at the age of 10 months) is classified into a favorable histology group. All markers are positive both in the cytoplasm and in the meshwork of neuropil. Neuropils are indicated by arrowheads. Immunohistochemical stainings (×400) for hTTL (*f*), Tyr-tubulin (*g*), Glu-tubulin (*h*), Δ2-tubulin (*i*) and TrkA (*j*) in an UH&A tumor. The tumor (neuroblastoma of undifferentiated subtype with a low mitosis-karyorrhexis index, diagnosed at the age of 21 months) is classified into an unfavorable histology group. Tumor cells lack neuropil formation and are uniformly negative for hTTL, Tyr-tubulin, Glu-tubulin and TrkA. Only Δ2-tubulin is detected in the cytoplasm of tumor cells (see Fig. 4*i*). Original magnification, ×400.

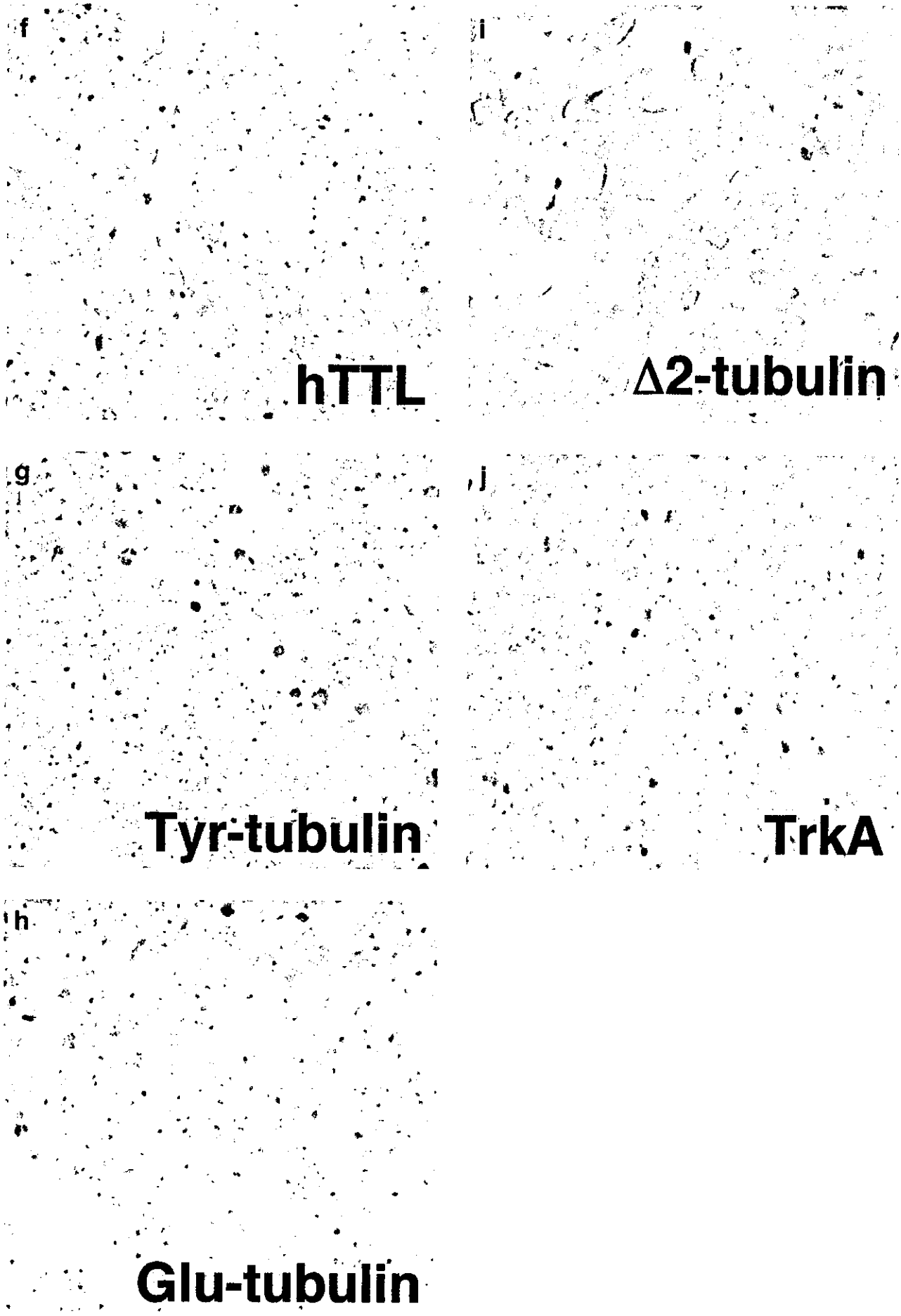

FIGURE 6 – (CONTINUED)

brain.[38] Therefore, many cellular stresses such as oxidative damage may trigger dysfunction of the tubulin/microtubule cytoskeletal system.

Our present study has shown that the decreases in Tyr-tubulin and Glu-tubulin are associated with relatively low levels of hTTL expression in unfavorable NBLs, which have lost a potency of neuronal differentiation and/or apoptosis. They are also correlated with decreased levels of TrkA, a high-affinity receptor for nerve growth factor, whose activation induces morphologic differentiation of NBL cells.[39] In addition, gradual upregulation of hTTL has been observed during induction of neuronal differentiation in RTBM1 cells treated with BMP2 or RA. These suggest that the induction of neuronal differentiation in NBL is accompanied with the activated tyrosination/detyrosination cycle regulated by increased level of hTTL enzyme, while the cycle is arrested by downregulation of hTTL in proliferating NBL cells, resulting in accumulation of Δ2-tubulin within the cells. Indeed, the expression levels of *hTTL* mRNA and Δ2-tubulin are significantly correlated with the prognosis of primary NBLs. This is consistent with the observation that TTL activity is lost, and conversely Δ2-tubulin is upregulated during the tumor cell growth.[19] Lafanechere *et al.*[19] have demonstrated by using mouse TTL null cells both *in vitro* and *in vivo* that mouse TTL activity is strongly decreased during tumor growth. Mas *et al.*[15] have also reported that, using rat *TTL* dominant negative mutant and an antisense cDNA of rat *TTL*, suppression of TTL activity induces 2- to 3-fold faster cell proliferation. Moreover, in human breast cancers, the accumulation of Glu-tubulin and Δ2-tubulin is correlated with poor prognosis by immunohistochemical approach.[28] It is noteworthy that our preliminary data using the microarray hybridized with total RNA obtained from 136 primary NBLs have shown that the gene with the highest score to predict prognosis of NBLs is α-tubulin (data not shown). Thus, the role of microtubule and its component, α-tubulin, is very important to define the biology as well as the aggressiveness of cancer cells.

In conclusion, we have identified a *human tubulin tyrosine ligase* gene and demonstrated its tissue distribution and correlation with neuronal differentiation. Since our data have suggested that the tyrosination cycle of α-tubulin is activated in differentiating NBLs but is inactivated in proliferating tumors, the cycle-related molecules including hTTL could be the targets for developing novel therapeutic strategies against advanced stages of NBL.

ACKNOWLEDGEMENTS

The authors thank Shigeru Sakiyama for critical reading of the manuscript, Naoko Sugimitsu for preparing RNA, Yuki Nakamura for DNA sequencing, Yoshiaki Okamoto for instructing quantitative real-time RT-PCR and Aiko Morohashi and Natsue Akao for technical assistance. The authors also thank the following institutions for providing surgical samples: First Department of Surgery, Hokkaido University School of Medicine; Department of Pediatrics, National Sapporo Hospital; Department of Pediatric Surgery, Tohoku University School of Medicine; Department of Surgery, Gunma Children's Medical Center; Department of Pediatrics, Pediatric Surgery and General Surgery, Jichi Medical University; Department of Hematology and Oncology, Saitama Children's Medical Center; Department of Pediatrics, Juntendo University School of Medicine; Department of Surgery, Kiyose Metropolitan Children's Hospital; Department of Surgery and Pathology, Chiba Children's Hospital; Department of Pediatric Surgery, Chiba University School of Medicine; Department of Pediatric Surgery, Kimitsu Central Hospital; Department of Pediatric Surgery, Niigata University School of Medicine; Department of Pediatrics and Pediatric Surgery, Aichi Medical University; Department of Pediatrics, Kyoto Prefectural Medical University; Tumor Board, Hyogo Children's Hospital; Department of Pediatrics and Pediatric Surgery, Kagoshima University School of Medicine; Department of Pediatric Surgery, Showa University School of Medicine; Department of Pediatrics, Oita University School of Medicine; Department of Pediatric Surgery, Ohta General Hospital; Department of Pediatrics, Ichinomiya City Hospital; Department of Pediatric Surgery, Osaka City General Hospital; Department of Pediatrics, Nihon University School of Medicine; Itabashi Hospital; Department of Pediatric Surgery, University of Tsukuba School of Medicine.

REFERENCES

1. MacRae TH. Tubulin post-translational modifications: enzymes and their mechanisms of action. Eur J Biochem 1997;244:265–78.
2. Zambito AM, Wolff J. Palmitoylation of tubulin. Biochem Biophys Res Commun 1997;239:650–4.
3. Barra HS, Arce CA, Argarana CE. Posttranslational tyrosination/detyrosination of tubulin. Mol Neurobiol 1988;2:133–53.
4. Luduena RF. Multiple forms of tubulin: different gene products and covalent modifications. Int Rev Cytol 1998;178:207–75.
5. Barra HS, Unates LE, Sayavedra MS, Caputto R. Capacities for binding amino acids by tRNAs from rat brain and their changes during development. J Neurochem 1972;19:2289–97.
6. Barra HS, Rodriguez JA, Arce CA, Caputto R. A soluble preparation from rat brain that incorporates into its own proteins (14 C)arginine by a ribonuclease-sensitive system and (14 C)tyrosine by a ribonuclease-insensitive system. J Neurochem 1973;20:97–108.
7. Barra HS, Arce CA, Rodriguez JA, Caputto R. Incorporation of phenylalanine as a single unit into rat brain protein: reciprocal inhibition by phenylalanine and tyrosine of their respective incorporations. J Neurochem 1973;21:1241–51.
8. Barra HS, Arce CA, Rodriguez JA, Caputto R. Some common properties of the protein that incorporates tyrosine as a single unit and the microtubule proteins. Biochem Biophys Res Commun 1974;60:1384–90.
9. Arce CA, Rodriguez JA, Barra HS, Caputo R. Incorporation of L-tyrosine, L-phenylalanine and L-3,4-dihydroxyphenylalanine as single units into rat brain tubulin. Eur J Biochem 1975;59:145–9.
10. Argarana CE, Arce CA, Barra HS, Caputto R. *In vivo* incorporation of [14C]tyrosine into the C-terminal position of the alpha subunit of tubulin. Arch Biochem Biophys 1977;180:264–8.
11. Preston SF, Deanin GG, Hanson RK, Gordon MW. The phylogenetic distribution of tubulin:tyrosine ligase. J Mol Evol 1979;13:233–44.
12. Gabius HJ, Graupner G, Cramer F. Activity patterns of aminoacyl-tRNA synthetases, tRNA methylases, arginyltransferase and tubulin: tyrosine ligase during development and ageing of *Caenorhabditis elegans*. Eur J Biochem 1983;131:231–4.
13. Stieger J, Wyler T, Seebeck T. Partial purification and characterization of microtubular protein from *Trypanosoma brucei*. J Biol Chem 1984;259:4596–602.
14. Ersfeld K, Wehland J, Plessmann U, Dodemont H, Gerke V, Weber K. Characterization of the tubulin-tyrosine ligase. J Cell Biol 1993;120:725–32.
15. Mas CR, Arregui CO, Filiberti A, Argarana CE, Barra HS. Cloning of rat olfactory bulb tubulin tyrosine ligase cDNA: a dominant negative mutant and an antisense cDNA increase the proliferation rate of cells in culture. Neurochem Res 2002;27:1453–8.
16. Paturle-Lafanechere L, Edde B, Denoulet P, Van Dorsselaer A, Mazarguil H, Le Caer JP, Wehland J, Job D. Characterization of a major brain tubulin variant which cannot be tyrosinated. Biochemistry 1991;30:10523–8.
17. Paturle-Lafanechere L, Manier M, Trigault N, Pirollet F, Mazarguil H, Job D. Accumulation of delta 2-tubulin, a major tubulin variant that cannot be tyrosinated, in neuronal tissues and in stable microtubule assemblies. J Cell Sci 1994;107:1529–43.
18. Lafanechere L, Job D. The third tubulin pool. Neurochem Res 2000;25:11–8.
19. Lafanechere L, Courtay-Cahen C, Kawakami T, Jacrot M, Rudiger M, Wehland J, Job D, Margolis RL. Suppression of tubulin tyrosine ligase during tumor growth. J Cell Sci 1998;111:171–81.
20. Ohira M, Morohashi A, Inuzuka H, Shishikura T, Kawamoto T, Kageyama H, Nakamura Y, Isogai E, Takayasu H, Sakiyama S, Suzuki Y, Sugano S, Goto T, Sato S, Nakagawara A. Expression profiling and characterization of 4200 genes cloned from primary neuroblastomas: identification of 305 genes differentially expressed between favorable and unfavorable subsets. Oncogene 2003;22:5525–36.
21. Ohira M, Morohashi A, Nakamura Y, Isogai E, Furuya K, Hamano S, Machida T, Aoyama M, Fukumura M, Miyazaki K, Suzuki Y, Sugano S, Hirato J, Nakagawara A. Neuroblastoma oligo-capping cDNA

project: toward the understanding of the genesis and biology of neuroblastoma. Cancer Lett 2003;197:63–8.
22. Brodeur GM, Pritchard J, Berthold F, Carlsen NL, Castel V, Castelberry RP, De Bernardi B, Evans AE, Favrot M, Hedborg F, kaneko M, Kemshead J, Lampert F, Lee RE, Look AT, Pearson AD, Philip T, Roald B, Sawada T, Seeger RC, Thuchida Y, Voute PA. Revisions of the international criteria for neuroblastoma diagnosis, staging, and response to treatment. J Clin Oncol 1993;11:1466–77.
23. Kaneko M, Nishihira H, Mugishima H, Ohnuma N, Nakada K, Kawa K, Fukuzawa M, Suita S, Sera Y, Tsuchida Y. Stratification of treatment of stage 4 neuroblastoma patients based on N-myc amplification status: Study Group of Japan for Treatment of Advanced Neuroblastoma, Tokyo, Japan. Med Pediatr Oncol 1998;31:1–7.
24. Hishiki T, Nimura Y, Isogai E, Kondo K, Ichimiya S, Nakamura Y, Ozaki T, Sakiyama S, Hirose M, Seki N, Takahashi H, Ohnuma N, Tanabe M, Nakagawara A. Glial cell line-derived neurotrophic factor/neurturin-induced differentiation and its enhancement by retinoic acid in primary human neuroblastomas expressing c-Ret, GFR alpha-1, and GFR alpha-2. Cancer Res 1998;58:2158–65.
25. Chomczynski P, Sacchi N. Single-step method of RNA isolation by acid guanidinium thiocyanate-phenol-chloroform extraction. Anal Biochem 1987;162:156–9.
26. Shimada H, Ambros IM, Dehner LP, Hata J, Joshi VV, Roald B, Stram DO, Gerbing RB, Lukens JN, Matthay KK, Castleberry RP. The International Neuroblastoma Pathology Classification (the Shimada system). Cancer 1999;86:364–72.
27. Goto S, Umehara S, Gerbing RB, Stram DO, Brodeur GM, Seeger RC, Lukens JN, Matthay KK, Shimada H. Histopathology (International Neuroblastoma Pathology Classification) and MYCN status in patients with peripheral neuroblastic tumors: a report from the Children's Cancer Group. Cancer 2001;92:2699–708.
28. Mialhe A, Lafanechere L, Treilleux I, Peloux N, Dumontet C, Bremond A, Panh MH, Payan R, Wehland J, Margolis RL, Job D. Tubulin detyrosination is a frequent occurrence in breast cancers of poor prognosis. Cancer Res 2001;61:5024–7.
29. Iwasaki S, Hattori A, Sato M, Tsujimoto M, Kohno M. Characterization of the bone morphogenetic protein-2 as a neurotrophic factor: induction of neuronal differentiation of PC12 cells in the absence of mitogen-activated protein kinase activation. J Biol Chem 1996;271:17360–5.
30. Nakamura Y, Ozaki T, Koseki H, Nakagawara A, Sakiyama S. Accumulation of p27 KIP1 is associated with BMP2-induced growth arrest and neuronal differentiation of human neuroblastoma-derived cell lines. Biochem Biophys Res Commun 2003;307:206–13.
31. Arregui CO, Mas CR, Argarana CE, Barra HS. Tubulin tyrosine ligase: protein and mRNA expression in developing rat skeletal muscle. Dev Growth Differ 1997;39:167–78.
32. Eiserich JP, Estevez AG, Bamberg TV, Ye YZ, Chumley PH, Beckman JS, Freeman BA. Microtubule dysfunction by posttranslational nitrotyrosination of alpha-tubulin: a nitric oxide-dependent mechanism of cellular injury. Proc Natl Acad Sci USA 1999;96:6365–70.
33. Kalisz HM, Erck C, Plessmann U, Wehland J. Incorporation of nitrotyrosine into alpha-tubulin by recombinant mammalian tubulin-tyrosine ligase. Biochim Biophys Acta 2000;1481:131–8.
34. Bisig CG, Purro SA, Contin MA, Barra HS, Arce CA. Incorporation of 3-nitrotyrosine into the C-terminus of alpha-tubulin is reversible and not detrimental to dividing cells. Eur J Biochem 2002;269:5037–45.
35. Ischiropoulos H. Biological tyrosine nitration: a pathophysiological function of nitric oxide and reactive oxygen species. Arch Biochem Biophys 1998;3561–611.
36. Hensley K, Maidt ML, Yu Z, Sang H, Markesbery WR, Floyd RA. Electrochemical analysis of protein nitrotyrosine and dityrosine in the Alzheimer brain indicates region-specific accumulation. J Neurosci 1998;18:8126–32.
37. Beal MF, Ferrante RJ, Browne SE, Matthews RT, Kowall NW, Brown RH Jr. Increased 3-nitrotyrosine in both sporadic and familial amyotrophic lateral sclerosis. Ann Neurol 1997;42:644–54.
38. Ishida Y, Ichimura T, Sumi H, Horigome T, Omata S. Methylmercury alters the tyrosination status of tubulin in the brains of acutely intoxicated rats. Toxicology 1997;122:171–81.
39. Nakagawara A, Arima-Nakagawara M, Scavarda NJ, Azar CG, Cantor AB, Brodeur GM. Association between high levels of expression of the TRK gene and favorable outcome in human neuroblastoma. N Engl J Med 1993;328:847–54.

Microbiol. Immunol., 49(1), 49–56, 2005

A Calcium Binding Protein, S100A4, Mediates T Cell Dependent Cytotoxicity as a Transformation-Associated Antigen

Nobuhiko Kondo[1], Shingo Ichimiya[1], Yasuaki Tamura[1], Akiko Tonooka[1], Shigeru Koshiba[1], Toshihiko Torigoe[1], Kenjiro Kamiguchi[1], Keizo Takenaga[2], and Noriyuki Sato*[,1]

[1]*Department of Pathology, Sapporo Medical University School of Medicine, Sapporo, Hokkaido 060–8556, Japan, and* [2]*Division of Chemotherapy, Chiba Cancer Center Research Institute, Chiba, Chiba 260–0801, Japan*

Received June 28, 2004; in revised form, October 23, 2004. Accepted October 28, 2004

Abstract: **The nature of the target molecule of TCRγδ T cell-mediated lysis remains to be determined. As we previously reported, #067 monoclonal antibody (mAb) recognizes one of the transformation-associated antigens, designated as #067 antigen. This antigen is expressed on the cell surface of rat fibrosarcoma W31 cells, which are established by transformation of fetal fibroblastic WFB cells with H-ras oncogene. It has been suggested that the #067 antigen is a target molecule for TCRγδ T cells since #067 mAb inhibited TCRγδ T cell-mediated lysis against #067 positive cells. In this study we attempted to identify the protein sequence of the #067 antigen. By using molecular cloning techniques, we demonstrated that a calcium binding protein, S100A4, was possibly one and the same molecule as the #067 antigen. It was shown that the expression of S100A4 was higher in W31 cells than in WFB cells at transcription and protein level. Flow cytometry and immunocytochemical studies showed that #067 antigen partially co-localized with S100A4 on the cell surface as well as the cytoplasm of W31 cells. Moreover, rabbit anti-S100A4 polyclonal antibodies (pAb) inhibited TCRγδ T cell-mediated lysis against #067 positive cells. Our results indicated that S100A4 may play a role as a possible target molecule for TCRγδ T cell-mediated lysis although how S100A4 is involved in TCRγδ T cell-mediated lysis remains to be determined.**

Key words: **TCRγδ, ras oncogene, S100A4, Transformation associated antigen**

Our previous studies have shown that a #067 monoclonal antibody (mAb)-defined molecule is a possible heat shock cognate protein and expressed on the cell surface of the rat fibroblast line W31, which has undergone malignant transformation by transfection with activated H-ras oncogene (19). This molecule is recognized by CD3(+), CD4(−), CD8(−), TCRαβ(−), and NKR-P1(−) double negative T (DNT) cells in an MHC-unrestricted manner, leading to target cell lysis (33). Furthermore, we have kept studying these T cells by establishing T cell hybridomas between these T cells and mouse BW5147 cells. The data indicated that the TCR usage of these T cells was determined preferentially, using the Vδ6 family and either the Vγ1 or the Vγ2 family (15, 17).

In this study, we performed cDNA expression cloning using human embryo kidney 293 (HEK293) cells and found that S100A4 was possibly one and the same molecule as the #067 antigen. S100A4 is reported to be a 10 kDa Ca-binding, cytoplasmic protein. This protein takes the forms of a homodimer and some heterodimers and is involved in tumor metastasis. However, a rabbit anti-S100A4 polyclonal antibodies (pAb) as well as a #067 mAb inhibited TCRγδ T cell-mediated lysis against target cells expressing #067 antigen. Therefore, our data suggests that S100A4 protein is a possible target for TCRγδ T cells. To our knowledge, this is the first report of a possible novel function of the S100A4 protein in the mechanism of TCRγδ T cell-mediated lysis.

Materials and Methods

Cells and antibodies. A WKA rat fetus-derived

**Address correspondence to* Dr. Noriyuki Sato, Department of Pathology, Sapporo Medical University School of Medicine, South-1, West-17, Chuo-ku, Sapporo, Hokkaido 060–8556, Japan. Fax: +81–11–643–2310. E-mail: satoh@sapmed.ac.jp

Abbreviations: BSA, bovine serum albumin; RNK16, rat NK lymphoma cell line; TCR, T cell receptor; WFB, Wistar-K-rat fibroblast cell line; W31, H-ras transformant of WFB.

fibroblast cell line, WFB, was used. W31 cells are transformant clones generated by the transfection of activated H-ras oncogene into WFB, as reported previously (17, 29). These cells and HEK293 cells were maintained in DMEM supplemented with 10% heat-inactivated fetal calf serum, 100 U/ml penicillin, and 100 μg/ml streptomycin in a humidified atmosphere at 37 C and 5% CO_2. RNK16 cells, an F344 rat-derived lymphoma cell line, and W31 constitutively express the #067 mAb-defined molecule on the cell surface, and both are sensitive to cytotoxicity by DNT cells. The sensitivity is MHC unrestricted and blocked by treatment with #067 mAb (17). FT126.1 is one of the TCRγδ T cell hybridomas we previously established and described (17). These two cell lines were cultured in RPMI-1640 containing 10% heat-inactivated fetal calf serum, 100 U/ml penicillin, and 100 μg/ml streptomycin in a humidified atmosphere at 37 C and 5% CO_2. #067 mAb had been previously generated to detect the transformation-associated antigen expressed on the cell surface of W31 (19). Rabbit anti-S100A4 pAb were employed for immunocytochemistry (31).

Construction of W31 cDNA library and expression cloning. Total RNA was extracted from approximately 1×10^8 W31 cells using Trizol (Invitrogen, Carlsbad, Calif., U.S.A.) according to the manufacturer's protocol. Next poly(A)+ selection by two rounds of chromatography on oligo(dT) cellulose was performed to obtain mRNA (Oligotex-dT 30 Super Kit; Roche, Basel, Switzerland). Integrity of the purified mRNA was assessed by formaldehyde-agarose gel electrophoresis. A cDNA library was synthesized using pCMV-Script XR Library Construction Kit (Stratagene, La Jolla, Calif., U.S.A.) and inserted into mammalian expression vector pCMV-Script at the *Eco*RI and *Xho*I sites, which were transformed into DH10B (Invitrogen) cells by electroporation. For the first screening, 600 pools of cDNAs constituted from 250 transformed DH10B cells were prepared. For the second screening, 20 pools of cDNAs constituted from 25 cells were prepared. For the last screening, 60 cDNA pools constituted from a single clone were prepared.

1×10^6 of HEK293 cells grown on 22 mm round glass coverslips pretreated with Collagen I (BIOCOAT; BD Biosciences, Bedford, Mass., U.S.A.) at approximately 80% confluency were transfected by Lipofectamine 2000 (Invitrogen) with cDNAs obtained from the amplified library. Forty-eight hours after transfection, the cells were harvested and immunoselection was performed. In brief, cells were fixed with ice-cold acetone and stained with #067 mAb, followed by incubation with Alexa 594 (red)-conjugated goat anti-mouse IgG (Molecular Probes, Eugene, Ore., U.S.A.). They were examined with laser scanning confocal microscopy (MRC1024; Bio-Rad, Hercules, Calif., U.S.A.). cDNAs were extracted from the transformed cells and transfected into competent cell, DH5α (TOYOBO, Osaka, Japan). Transformed cells were cultured in NZCYM broth medium (Invitrogen), and cDNAs were prepared using QIAfilter Plasmid Maxi Kit (QIAGEN, Valencia, Calif., U.S.A.) for subsequent transfection.

Immunocytochemistry. Cells cultured on BIOCOAT were fixed with ice-cold acetone and stained with #067 mAb, followed by reaction with Alexa 594 (red)-conjugated goat anti-mouse IgG. For double-staining analysis, cells on BIOCOAT were subjected to staining with #067 mAb and rabbit anti-S100A4 pAb. These were visualized with Alexa 488 (green)-conjugated goat anti-mouse IgG and Alexa 594 (red)-conjugated goat anti-rabbit IgG, respectively and examined with a laser scanning confocal microscope (MRC1024; Bio-Rad).

Northern hybridization. Total RNA was isolated by a single step RNA isolation method using Trizol according to the manufacturer's protocol. Ten micrograms of total RNA was separated by electrophoresis through 1% formalin gel and transferred onto Hybond-N+ membranes (Amersham Pharmacia Biotech, Uppsala, Sweden). Hybridization was performed as specified in the manufacturer's protocol using ExpressHyb solution (Clontech, Palo Alto, Calif., U.S.A.). Briefly, the membrane filter was hybridized with radiolabeled probes at 68 C for 15 hr. Then the filter was washed in SSC containing 0.1% SDS solution with stepwise decreased salt concentrations followed by 2× SSC, 1× SSC, and 0.5× SSC at 50 C for 30 min. The filter was subjected to autoradiography for consecutive days to a maximum of one month.

The cDNA probe for detecting S100A4 transcripts was generated by the RT-PCR method on cDNA of W31 cells with specific primers for S100A4 cDNA (S100A4 forward primer: 5'-TCAGCACTTCCTCTCTCTTG-3', S100A4 reverse primer: 5'-CAGCCAACATGGAAGATTCG-3'). The amplified products, 397 bp in length, were ligated into pGEM-T easy vector (Promega, Madison, Wis., U.S.A.) and the nucleotide sequence of the insert DNA was confirmed using an ABI-PRISM 310 sequencer (PE Applied Biosystems, Foster City, Calif., U.S.A.). The labeling of the insert DNA digested with *Eco*RI and hybridization were performed as described above.

Western blot analysis. Cell lysis was performed using subconfluent cultures by incubating 10 cm^2 dishes with 1 ml of lysis buffer containing 0.5% NP-40, 10 mM Tris-HCl (pH 7.4), 150 mM NaCl, 1 mM EDTA and protease inhibitors (Roche) for 30 min at 4 C as previously described (14). Aliquots of the supernatants were